Journal Pre-proofs

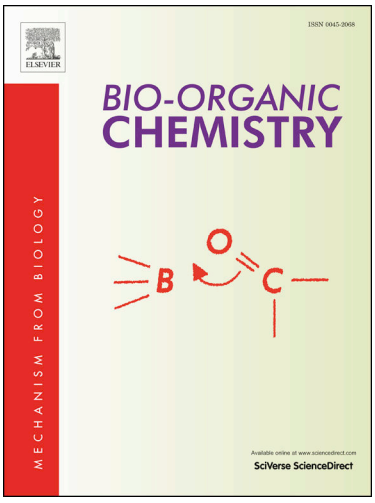

Functionalization of 9-thioxanthone at the 1-position: from arylamino derivatives to [1]benzo(thio)pyrano[4,3,2-de]benzothieno[2,3-b]quinolines of biological interest

Nahida Mokhtari Brikci-Nigassa, Lionel Nauton, Pascale Moreau, Olivier Mongin, Raphaël Duval, Laurent Picot, Valérie Thiéry, Mohamed Souab, Sandrine Ruchaud, Stéphane Bach, Rémy Le Guevel, Ghenia Bentabed-Ababsa, William Erb, Thierry Roisnel, Vincent Dorcet, Florence Mongin

PII: S0045-2068(19)31210-6
DOI: https://doi.org/10.1016/j.bioorg.2019.103347
Reference: YBIOO 103347

To appear in: *Bioorganic Chemistry*

Received Date: 27 July 2019
Revised Date: 3 October 2019
Accepted Date: 4 October 2019

Please cite this article as: N. Mokhtari Brikci-Nigassa, L. Nauton, P. Moreau, O. Mongin, R. Duval, L. Picot, V. Thiéry, M. Souab, S. Ruchaud, S. Bach, R. Le Guevel, G. Bentabed-Ababsa, W. Erb, T. Roisnel, V. Dorcet, F. Mongin, Functionalization of 9-thioxanthone at the 1-position: from arylamino derivatives to [1]benzo(thio)pyrano[4,3,2-de]benzothieno[2,3-b]quinolines of biological interest, *Bioorganic Chemistry* (2019), doi: https://doi.org/10.1016/j.bioorg.2019.103347

Graphical Abstract

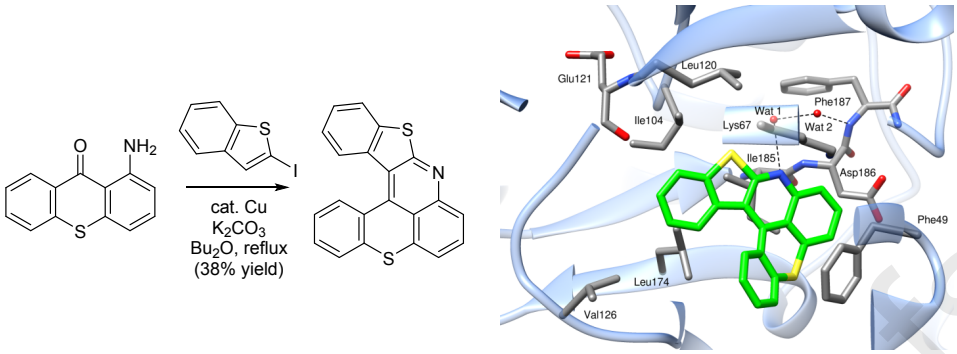

Functionalization of 9-thioxanthone at the 1-position: from arylamino derivatives to [1]benzo(thio)pyrano[4,3,2-*de*]benzothieno[2,3-*b*]quinolines of biological interest

Nahida Mokhtari Brikci-Nigassa,[a,b] Lionel Nauton,[c] Pascale Moreau,[c,*] Olivier Mongin,[a]

Raphaël Duval,[d] Laurent Picot,[e] Valérie Thiéry,[e] Mohamed Souab,[f] Sandrine Ruchaud,[f,g]

Stéphane Bach,[f,g,*] Rémy Le Guevel,[h] Ghenia Bentabed-Ababsa,[b,*] William Erb,[a]

Thierry Roisnel,[a] Vincent Dorcet,[a] Florence Mongin[a,*]

[a] *Univ Rennes, CNRS, ISCR (Institut des Sciences Chimiques de Rennes) - UMR 6226, F-35000 Rennes, France*

[b] *Laboratoire de Synthèse Organique Appliquée, Faculté des Sciences Exactes et Appliquées, Université Oran1 Ahmed Ben Bella, BP 1524 El M'Naouer, 31000 Oran, Algeria*

[c] *Université Clermont Auvergne, CNRS, SIGMA Clermont, ICCF, F-63000 Clermont-Ferrand, France*

[d] *Université de Lorraine, CNRS, L2CM, F-54506 Nancy, France*

[e] *Laboratoire Littoral Environnement et Sociétés, UMRi CNRS 7266, La Rochelle Université, 17042 La Rochelle, France*

[f] *Sorbonne Université, CNRS, FR2424, Plateforme de criblage KISSf (Kinase Inhibitor Specialized Screening facility), Station Biologique de Roscoff, Place Georges Teissier, 29682 Roscoff, France*

[g] *Sorbonne Université, CNRS, UMR 8227, Integrative Biology of Marine Models, Station Biologique de Roscoff, CS 90074, 29688 Roscoff Cedex, France*

[h] *Univ Rennes, Plateforme ImPACcell, SFR BIOSIT - UMS CNRS 3480, UMS INSERM 018, F-35000 Rennes, France*

* Corresponding authors.
E-mail addresses: pascale.moreau@uca.fr (P. Moreau), bach@sb-roscoff.fr (S. Bach), badri_sofi@yahoo.fr (G. Bentabed-Ababsa), florence.mongin@univ-rennes1.fr (F. Mongin).

Keywords: thioxanthone; *N*-arylation; copper; kinase inhibition; melanoma cells; fluorescence

Abstract:

Original 1-amino substituted thioxanthone derivatives were easily prepared from the bare heterocycle by a deprotometalation-iodolysis-copper-catalyzed C-N bond formation sequence. This last reaction delivered mono- or/and diarylated products depending on the aniline involved. 1-Amino-9-thioxanthone was also prepared and reacted with 2-iodoheterocycles. Interestingly, while 1-(arylamino)-9-thioxanthones could be isolated, their subsequent cyclization was found to deliver original hexacyclic derivatives of helicoidal nature. Evaluation of their photophysical properties revealed high fluorescence in polar media, indicating potential applications for biological imaging. These compounds being able to inhibit PIM1 kinase, their putative binding mode was examined through molecular modeling experiments. Altogether, these results tend to suggest the discovery of a new family of fluorescent PIM inhibitors and pave the way for their future rational optimization.

1. Introduction

Thioxanthones are part of the aromatic heterocycles found in bioactive compounds (Figure 1). Lucanthone is for example a DNA intercalating derivative that inhibits the synthesis of macromolecules by interfering with the activity of topoisomerase I and II during replication and transcription. It specifically inhibits the DNA repair enzyme apurinic/apyrimidinic endodeoxyribonuclease 1 in a way that results in unrepaired DNA strand breaks, possibly inducing apoptosis and reducing tumor cell resistance to radio- and chemotherapy. It also disrupts lysosomal function, inhibiting autophagy. Both lucanthone and its metabolite hycanthone show antischistosomal and antineoplastic activities. The analogues SR233377 and SR271425 are also cytotoxic DNA-interacting agents that exhibit a broad antitumor activity. However, the side effects of all these compounds - mutagenicity (e.g. in the case of lucanthone and hycanthone, due to the methylene moiety linked to their 4-position) or cardiotoxicity (e.g. for SR271425) - made clinical use impossible [1]. Investigations are still ongoing in order to identify more selective antitumor agents [2, 3].

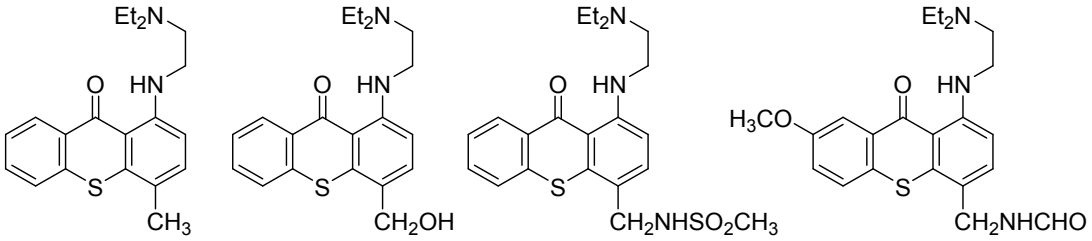

Figure 1. Examples of thioxanthone derivatives possessing biological properties.

In the course of a previous work, we identified the easily accessible thioxanthone derivative **HM107-g** as a potent antibacterial and antifungal agent without significant toxicity on human red blood cells (Figure 2). In addition, upon evaluation against a short panel of serine/threonine protein kinases, this compound inhibited human proto-oncogene PIM1 with an IC_{50} value of 610 nM [4]. In continuation with this preliminary work, we report here the 2- or 3-step syntheses of 9-thioxanthone derivatives, as well as their photophysical and biological evaluation.

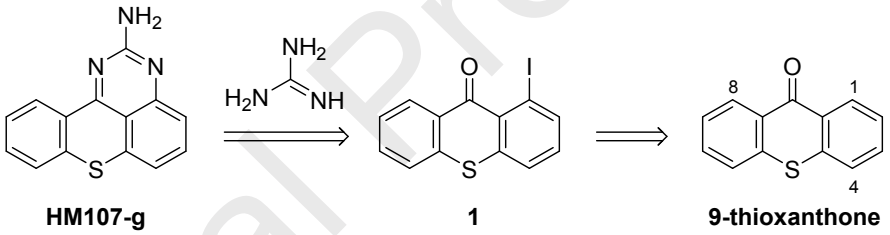

Figure 2. Retrosynthetic pathway of the PIM1 kinase inhibitor **HM107-g** [4].

2. Results and Discussion

2.1. Synthesis

The traditional approach to access 1-substituted 9-thioxanthones relies on intramolecular electrophilic cyclizations from suitably substituted benzoic acids or related compounds. Although able to deliver various derivatives, it generally requires harsh reaction conditions [1]. A few direct methods to functionalize the 1-position of 9-thioxanthone are documented, such as some ruthenium-catalyzed activations [5, 6], the rhodium-mediated reaction with maleimides [7] and the iridium-catalyzed oxidative heteroarylation with thiophene [8].

Both in order to avoid the use of an expensive transition metal and to reduce the competitive 1,8-difunctionalization sometimes noticed in the previous methodologies, we decided to employ cheaper reagents, and selected deprotometalation-trapping to access 1-halogeno 9-thioxanthones. Because 9-thioxanthone is a substrate prone to nucleophilic attack, it was deprotonated by using hindered lithium amide LiTMP (TMP = 2,2,6,6-tetramethylpiperidino) and $ZnCl_2$·TMEDA (TMEDA = *N*,*N*,*N'*,*N'*-tetramethylethylenediamine) as *in situ* trap [9], as reported previously [4, 10]. In THF (THF = tetrahydrofuran) at -30 °C, the deprotolithiation-transmetalation took place efficiently, as demonstrated by subsequent iodolysis to give the expected iodide in 84% yield (Scheme 1). Although the competitive formation of the diiodide **1'** could not be totally avoided (10% isolated yield), this side product was easily discarded by column chromatography over silica gel. It is worth noting that the corresponding bromide and chloride should be similarly synthesized [11]; however, the iodide appeared to be more reactive in the forthcoming copper-catalyzed C-N bond formation reactions.

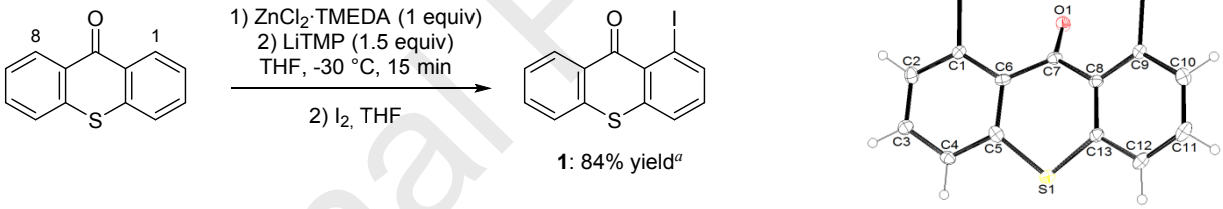

Scheme 1. Synthesis of 1-iodo-9-thioxanthone (**1**) and ORTEP diagram (50% probability) of the compound **1'**. [a] 1,8-Diiodo-9-thioxanthone (**1'**) was also isolated in 10% yield.

In order to benefit from the presence of both ketone function and adjacent iodine, we first considered reacting **1** with 1,2-phenylenediamine in order to access the benzodiazepine derivative **2a** (Figure 3). According to our previous work [12], amidation was performed from the iodo derivative **1** with catalytic copper(I) iodide and potassium carbonate in dimethylsulfoxide. However, only traces of the expected product **2a** were detected (identified only by X-ray diffraction; see Figure 3). The major product isolated was unambiguously identified as 1-(2-aminophenylamino)-9-thioxanthone (**2a'**), indicating a sluggish cyclization under these conditions. Using 2,3-diaminopyridine similarly led to **2b'**

(Scheme 2; Figure 3). The yields are moderate, due to competitive deiodination of **1** under the coupling reaction conditions.

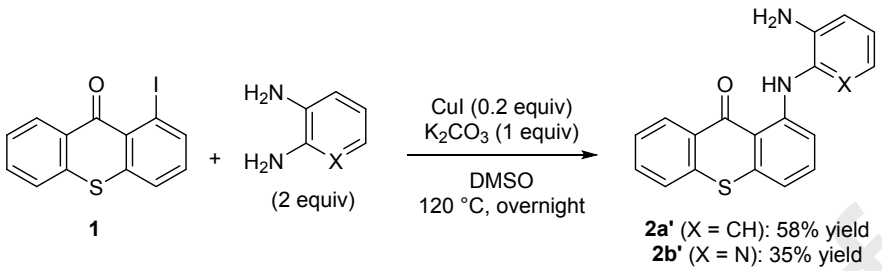

Scheme 2. Unsuccessful attempts to reach benzodiazepine-containing derivatives.

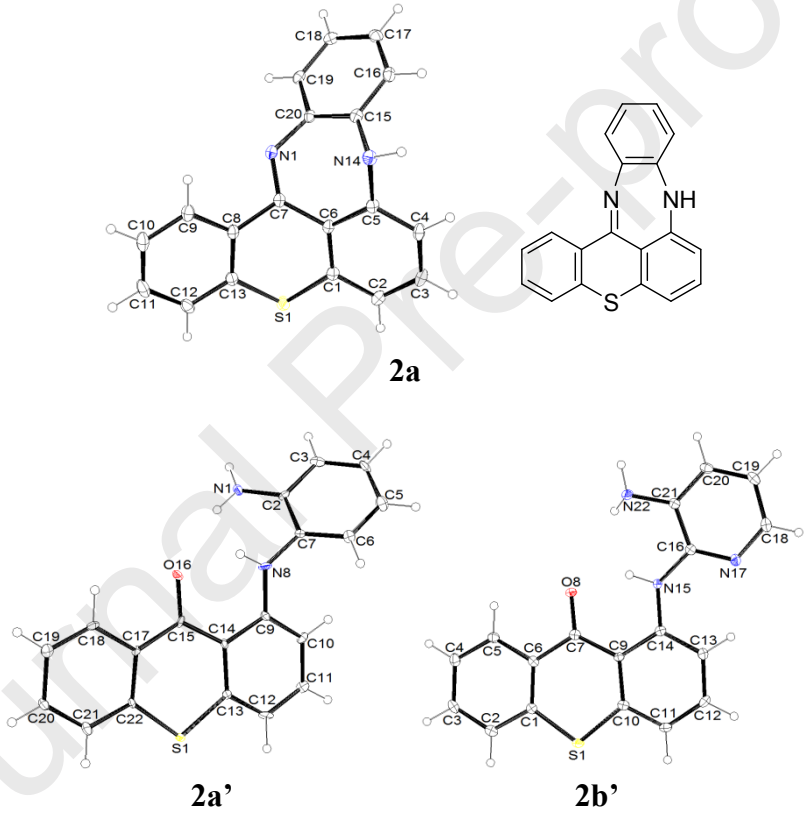

Figure 3. ORTEP diagrams (50% probability) of the compounds **2a**, **2a'** and **2b'**.

These results show that the formation of benzodiazepine-containing derivatives from **1** might be possible, but would require a comprehensive study. Therefore, we opted for the evaluation of simpler anilines. After a short optimization of the amounts of aniline, base and copper(I) iodide, and the reaction temperature and time, the conditions shown in Table 1 were applied to the *N*-arylation of 4-(trifluoromethylsulfonyl)-, 4-fluoro- and 4-methylaniline by **1**. The corresponding coupled products **3a-**

c were isolated in moderate yields due to the difficulty to separate them from deiodinated 9-thioxanthone or/and the bis-*N*-arylated product (entries 1-3; Figure 4). In the case of 4-methylaniline, this bis-*N*-arylated product **3c'** could be isolated and identified unambiguously (entry 3).

Table 1. *N*-arylation of different anilines using 1-iodo-9-thioxanthone (**1**).

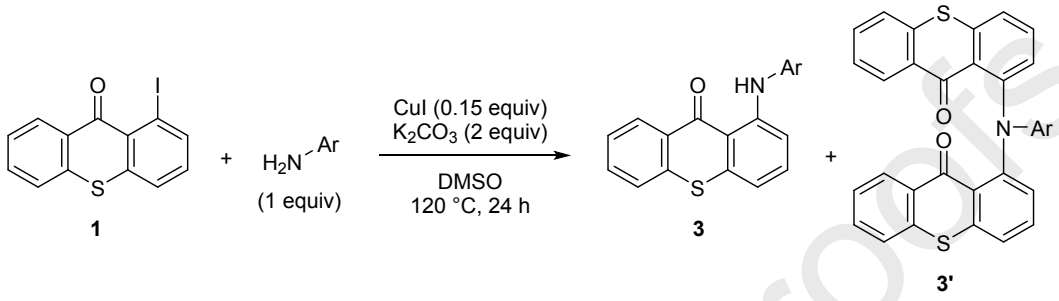

Entry	H_2N-Ar	**3**, Yield (%)[a]	**3'**, Yield (%)[a]
1	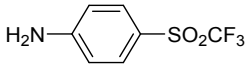	**3a**, 58	-[b]
2	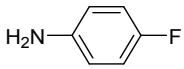	**3b**, 31	-[b]
3	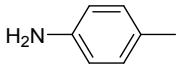	**3c**, 50[c]	**3c'**, 6
4	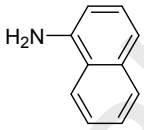	**3d**, 63	-[d]
5[e]		**3e**, <10[c]	**3e'**, 41

[a] After purification (see experimental part). [b] Not isolated (yield not estimated).
[c] Estimated yield due to purification issue. [d] Not found. [e] 0.5 equiv of 4-anisidine was used.

We noticed that the use of 1-naphthylamine did not lead to the bis-*N*-arylated compound (entry 4; Figure 4). This could be rationalized by a more important steric hindrance since it became the major product by reducing the amount of 4-methoxyaniline to 0.5 equivalent (entry 5). These results also suggest that using this ligandless catalytic system might favor bis-arylation. Indeed, competitive formation of triarylamines in the course of copper-catalyzed *N*-arylation of anilines has already been observed, but when substituted by electron-withdrawing groups [13, 14]; in the present case, triarylamines were even formed from electron-rich anilines. The bis-coupled products **3c'** and **3e'**

showed original crystal structures, with both heterocycles being quasi-stacked and arranged head-to-foot (Figure 4).

Inspired by the *N*-arylation of 1-amino-9-xanthone with 3-iodoanisole reported by Fujiwara and Kitagawa in 2000 [15], we attempted to use a mixture of activated copper and copper(I) iodide, and replaced dimethylsulfoxide by dimethylformamide. Under these conditions, 4-aminopyridine was reacted with **1** to afford the product **3f**, but still in a moderate yield (Scheme 3).

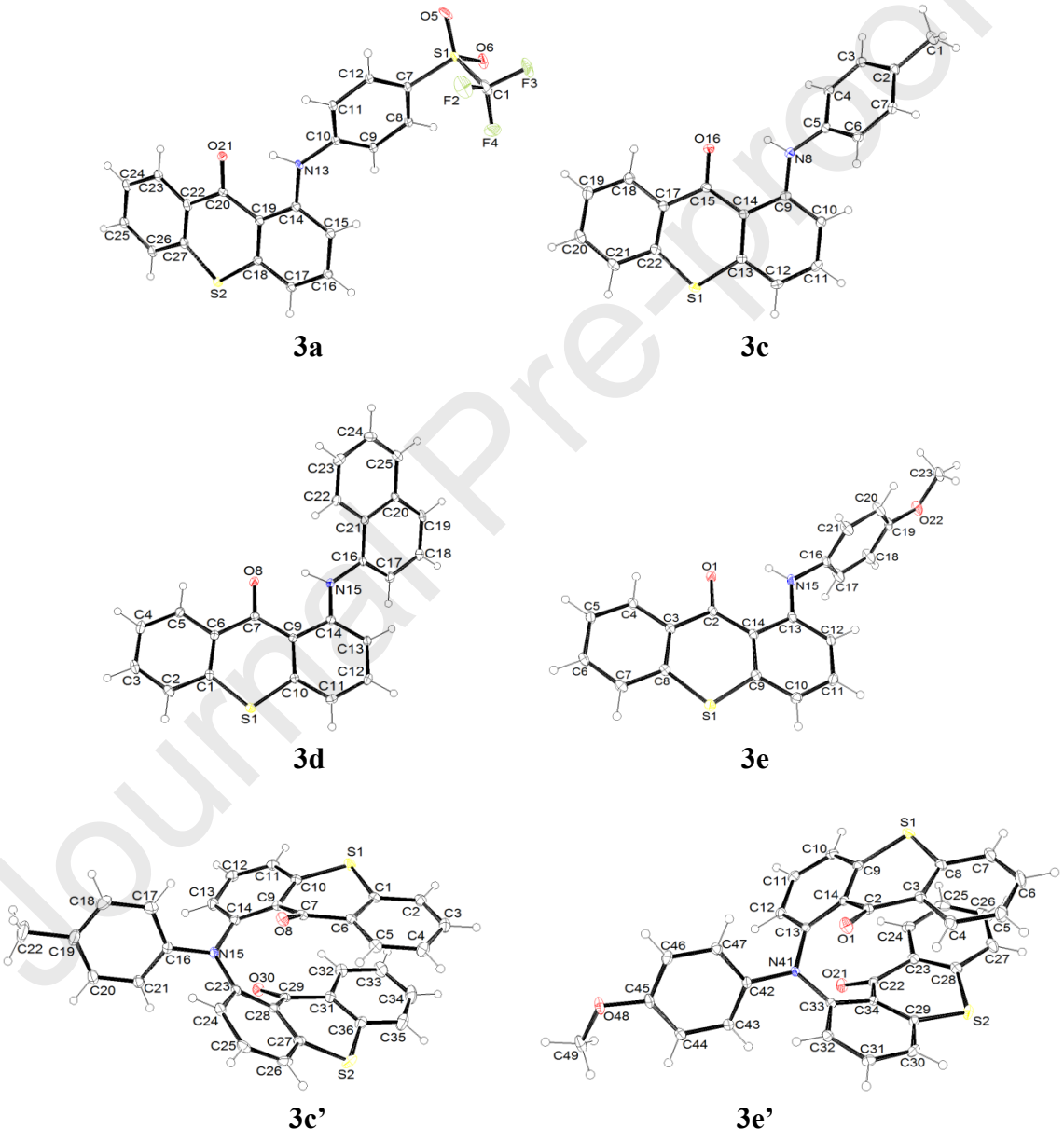

Figure 4. ORTEP diagrams (50% probability) of the compounds **3a**, **3c**, **3d**, **3e**, **3c'** and **3e'**.

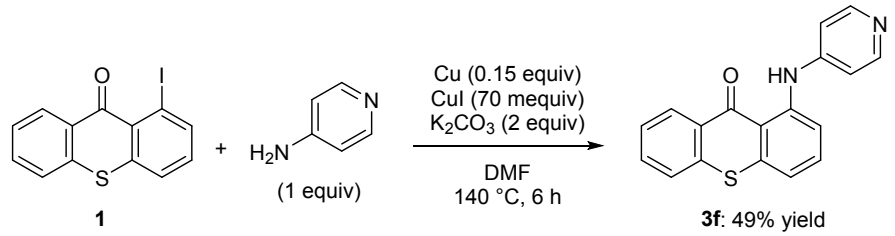

Scheme 3. *N*-arylation of 4-aminopyridine by using 1-iodo-9-thioxanthone (**1**).

We recently showed that, after *N*-arylation with 2-iodobenzofuran and 2-iodobenzothiophene, 2-aminophenones were instantly converted into the corresponding tetracycles, as depicted in Figure 5 [16]. As these derivatives showed promising antiproliferative activity in melanoma cells, we decided to prepare 1-amino-9-thioxanthone and attempt the corresponding reactions.

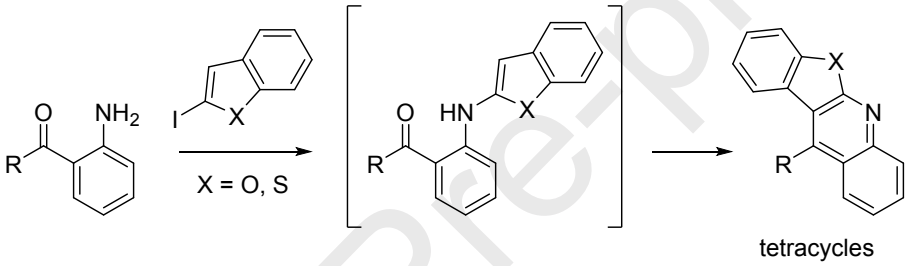

Figure 5. Synthetic pathway of tetracycles of biological interest [16].

A direct access to 1-amino-9-thioxanthone (**4**) was considered by amination of **1** according to various conditions reported in the literature for the synthesis of anilines from aryl iodides. First, inspired by Kim and Chang's protocol [17], we employed excess aqueous ammonia in the presence of copper(I) iodide (0.2 equiv), L-proline (0.4 equiv) and potassium carbonate (3 equiv) in dimethylsulfoxide; after 5 days at 80 °C, the expected amino derivative **4** was isolated in 44% yield (the rest was starting **1**). We next adapted a protocol from the work of Ji, Atherton and Page [18], and treated **1** by copper(I) chloride (0.1 equiv), sodium ascorbate (0.1 equiv) and excess ammonia in methanol; after 14 hours at 100 °C, the product **4** was isolated in 20% yield (the rest was 9-thioxanthone, formed by deiodination of **1**). Finally, we applied the protocol using copper(I) iodide (0.1 equiv), DMEDA (DMEDA = *N*,*N'*-dimethylethylenediamine; 0.15 equiv), excess aqueous ammonia and dimethylsulfoxide at 130 °C (sealed tube) reported by Jeon and co-workers [19]; after 16 hours at this temperature, the expected

amine **4** was isolated in 50% yield (Scheme 4). Under these conditions, although no degradation of **1** took place, the competitive formation of a fluorescent unidentified compound was noticed (possessing a singlet at ~9.1 ppm in its ^{1}H NMR spectra). Replacing DMEDA by PEG300 also gave **4**, but in a lower 33% yield.

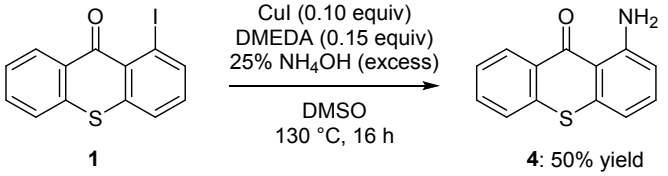

Scheme 4. Conversion of 1-iodo-9-thioxanthone (**1**) into 1-amino-9-thioxanthone (**4**).

We used the amine **4** with various substrates such as 2-iodothiophene, 2-iodobenzothiophene and 2-iodobenzofuran. In order to favor the formation of polycyclic molecules, we used conditions similar to those that afforded the tetracycles shown in Figure 5. Thus, the amine **4** was treated by the iodide in the presence of activated copper (0.2 equiv) and potassium carbonate (2 equiv) at the reflux temperature of dibutyl ether (Table 2).

Table 2. *N*-arylation of 1-amino-9-thioxanthone (**4**) by using heteroaryl iodides.

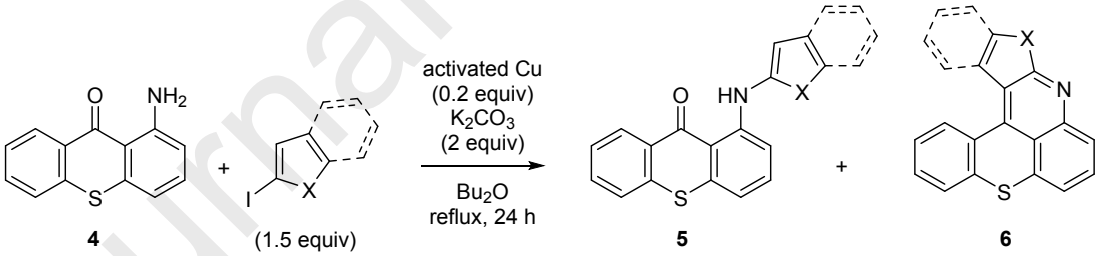

Entry	Heteroaryl iodide	**5**, Yield (%)[a]	**6**, Yield (%)[a]
1		**5a**, 40	-[b]
2	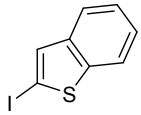	**5b**, 50	**6b**, 38
3	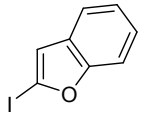	-[b]	**6c**, 21

[a] After purification (see experimental part). [b] Not searched.

After 24 hours, although hardly separable mixtures were obtained, careful chromatography afforded compounds **5** or/and **6**. In the case of 2-iodothiophene, the product **5a** resulting from a mono-*N*-arylation of **4** was isolated in 40% yield (entry 1). With 2-iodobenzothiophene, both **5b** and the cyclized product **6b** could be isolated (entry 2, respective yields of 50 and 38%; Figure 6). From 2-iodobenzofuran, the hexacycle **6c** was the only isolated product, obtained in a moderate 21% yield (entry 3; Figure 6). Unfortunately, our attempts to convert the *N*-arylated products **5** into the fluorescent products **6** by acid-mediated cyclization [20] only led to degradation. It was however interesting to study the luminescence properties of the compounds **6b** and **6c**.

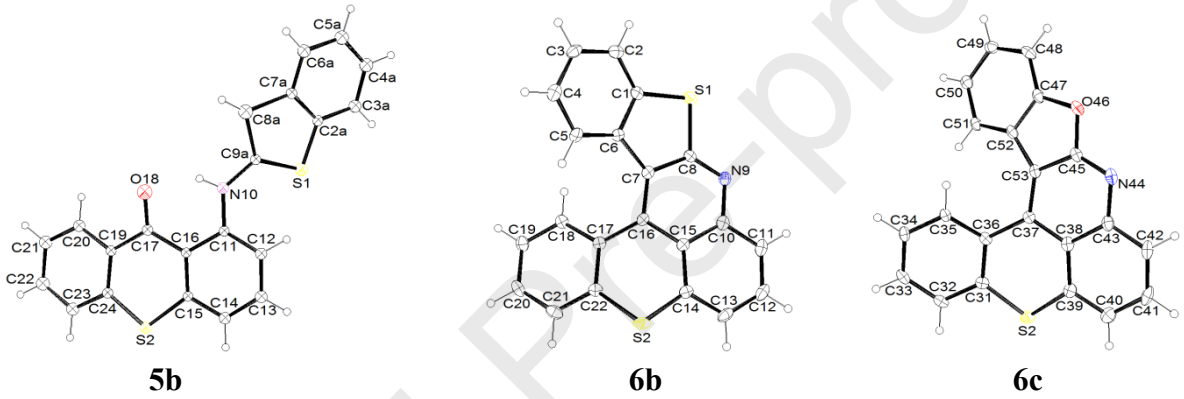

5b **6b** **6c**

Figure 6. ORTEP diagrams (50% probability) of the compounds **5b**, **6b** and **6c**.

2.2. Physicochemical properties

During the purification of the hexacyclic compounds **6b** and **6c**, we noticed their strong fluorescent behavior. Therefore, in view of potential applications as fluorescent probes in biological media, we initiated the early evaluation of their photophysical properties. Their absorption and emission properties were first investigated in toluene (Figure 7), and the results are gathered in Table 3.

Both compounds absorb in the blue-violet part of the visible region and emit in the green one. The replacement of the oxygen atom of **6c** with a sulfur atom (**6b**) leads to 12 nm and 20 nm bathochromic shift in absorption and emission, respectively. Their luminescence quantum yields are quite high and almost identical. Their luminescence lifetimes are in the range of 15 nanoseconds, which confirms that

this emission is indeed a fluorescence phenomenon. The radiative decay rate of **6c** is slightly higher than that of **6b** (in agreement with a concomitant increase of the molar extinction coefficient), but its nonradiative decay rate decreases almost similarly, which leads to the maintaining of the fluorescence quantum yield.

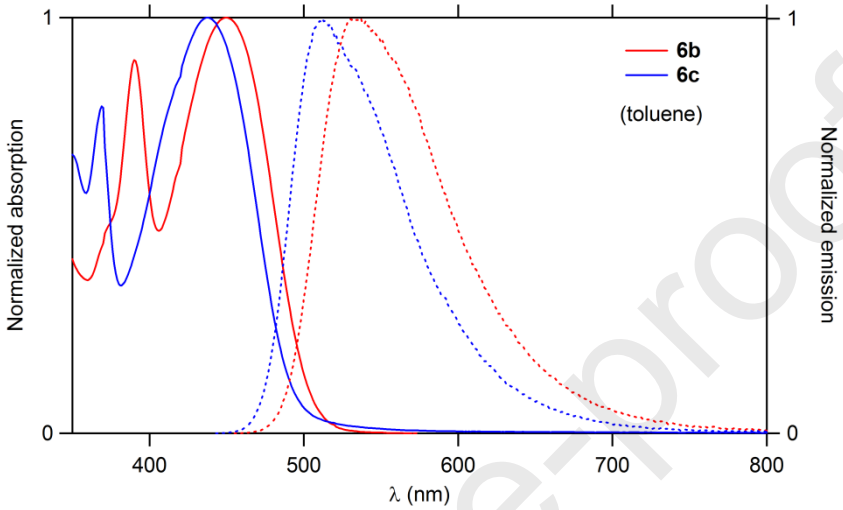

Figure 7. Absorption (solid line) and emission (dotted line) of compounds **6b** and **6c** in toluene.

Table 3. Absorption and emission properties of **6b** and **6c** in toluene at 25 °C.

Compound	λ_{abs} [a] (nm)	ε_{max} [b] (M^{-1} cm^{-1})	λ_{em} [c] (nm)	Φ_F [d]	τ [e] (ns)	k_r [f] (s^{-1})	k_{nr} [f] (s^{-1})
6b	449	6800	532	0.50	16.5	3.03×10^7	3.03×10^7
6c	437	8300	512	0.49	13.6	3.60×10^7	3.75×10^7

[a] Absorption maximum. [b] Molar extinction coefficient at λ_{abs}. [c] Emission maximum. [d] Fluorescence quantum yield using as a standard quinine bisulfate in 0.5 M H_2SO_4, upon excitation at λ_{abs}. [e] Fluorescence lifetime. [f] Radiative (k_r) and nonradiative (k_{nr}) decay rates derived from fluorescence quantum yield and lifetime values ($k_r = \Phi_F/\tau$; $k_{nr} = (1-\Phi_F)/\tau$).

The influence of the solvent polarity on the absorption and emission properties of the compounds **6b** (Figure 8 and Table 4) and **6c** (Figure 9 and Table 5) was then studied. Almost no solvatochromism was observed in absorption, whereas a positive (in agreement with the π-π* character of the lowest energy transition) but weak solvatochromic behavior was observed in emission for both compounds. More interestingly, their fluorescence quantum yield is also not very sensitive to the increase of the

solvent polarity, maintaining values higher than 40% in a polar solvent such as acetonitrile. This means that such compounds should remain fluorescent enough to monitor them in biological media.

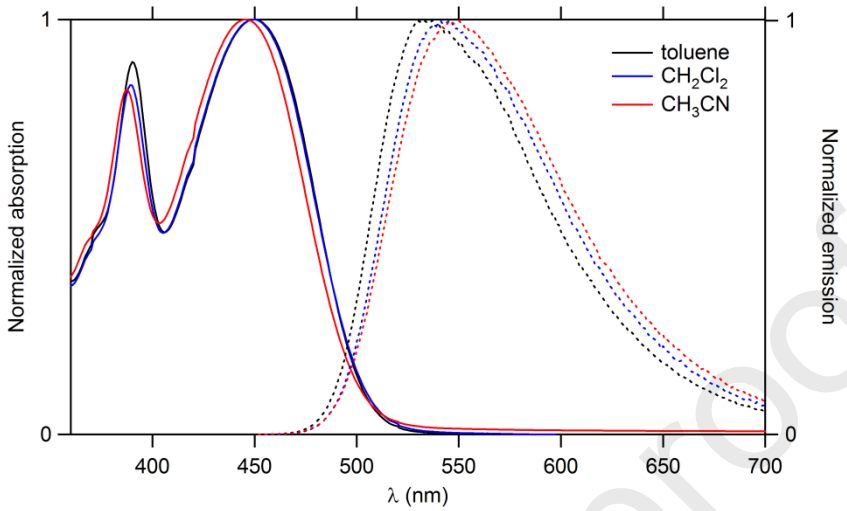

Figure 8. Absorption (solid line) and emission (dotted line) of compound **6b** in different solvents.

Table 4. Solvatochromic data of **6b** at 25 °C.

Solvent	λ_{abs} [a] (nm)	λ_{em} [b] (nm)	Φ_F [c]	Stokes shift (cm^{-1}) [d]
toluene	449	532	0.50	3470
CH_2Cl_2	449	542	0.56	3820
CH_3CN	446	549	0.42	4210

[a] Absorption maximum. [b] Emission maximum. [c] Fluorescence quantum yield using as a standard quinine bisulfate in 0.5 M H_2SO_4, upon excitation at λ_{abs}. [d] Stokes shift = $(1/\lambda_{abs} - 1/\lambda_{em})$.

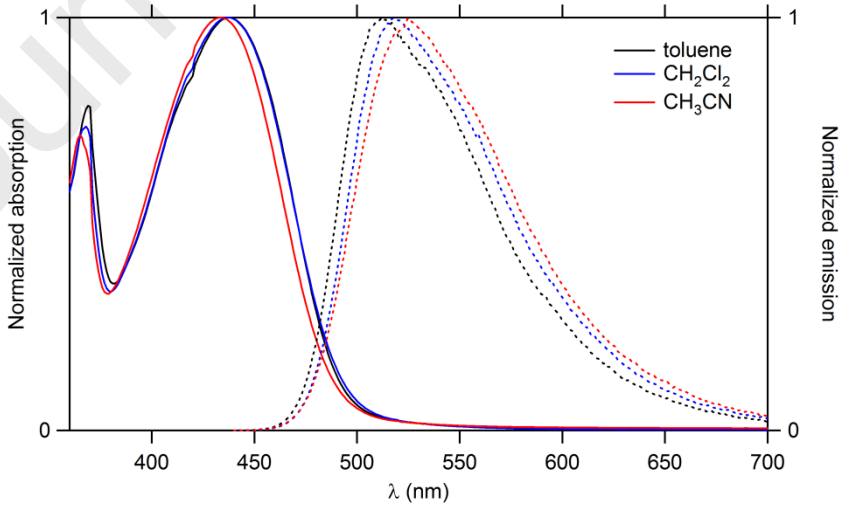

Figure 9. Absorption (solid line) and emission (dotted line) of compound **6c** in different solvents.

Table 5. Solvatochromic data of **6c** at 25 °C.

Solvent	λ_{abs} [a] (nm)	λ_{em} [b] (nm)	Φ_F [c]	Stokes shift (cm^{-1}) [d]
toluene	437	512	0.49	3350
CH_2Cl_2	437	518	0.56	3580
CH_3CN	434	525	0.42	3990

[a] Absorption maximum. [b] Emission maximum. [c] Fluorescence quantum yield using as a standard quinine bisulfate in 0.5 M H_2SO_4, upon excitation at λ_{abs}. [d] Stokes shift = $(1/\lambda_{abs} - 1/\lambda_{em})$.

2.3. Evaluation on kinases and molecular modeling experiments

Protein kinases which are often deregulated in diseases such as cancers and neurodegenerative disorders have become a major class of drug targets since the end of the nineties [21]. Today, 50 FDA-approved kinase inhibitors are on the market and many drug candidates are undergoing clinical evaluation [22, 23]. As part of our ongoing research on novel protein kinase inhibitors, some of the synthesized compounds were also evaluated [16] against a short panel of disease-related protein kinases: cyclin-dependent kinases 2 (CDK2/Cyclin A) and 9 (CDK9/Cyclin T), proto-oncogene kinase PIM1, CDC2-like kinase 1 (CLK1), dual specificity tyrosine phosphorylation regulated kinase 1A (DYRK1A), glycogen-synthase kinase-3 (GSK-3 isoforms α/β), casein kinase 1 (CK1 isoforms δ/ε) and mitotic kinase Haspin (Table 6).

Table 6. Inhibitory activities of synthesized compounds against a short panel of disease-related protein kinases. The table displays the remaining kinase activities detected after treatment with 10 µM of the tested compounds. The values obtained after treatment with 1 µM are given in brackets. Results are expressed in % of maximal activity, i.e. measured in the absence of inhibitor but with an equivalent dose of DMSO (solvent of the tested compounds). ATP concentration used in the kinase assays was 10 µmol/L (values are means, n = 2). Kinases are from human origin unless specified: *Mm*, *Mus musculus*; *Rn*, *Rattus norvegicus*; *Ssc*, *Sus scrofa domesticus*.

Compound	CDK2/CyclinA	CDK9/CyclinT	PIM1	*Mm*CLK1	*Rn*DYRK1A	*Ssc*GSK3α/β	*Ssc*CK1δ/ε	Haspin
2a'	106 (99)	79 (96)	104 (101)	105 (104)	141 (170)	103 (105)	85 (99)	98 (99)
3b	98 (109)	71 (80)	107 (107)	97 (104)	103 (146)	98 (109)	103 (124)	96 (104)
3c	95 (98)	100 (94)	110 (100)	81 (101)	68 (71)	86 (89)	84 (102)	87 (98)
3c'	103 (91)	56 (61)	105 (97)	106 (97)	124 (109)	101 (75)	112 (98)	114 (91)
3e	93 (82)	77 (84)	98 (88)	95 (101)	107 (94)	100 (96)	92 (97)	77 (100)
5b	95 (92)	81 (103)	106 (99)	108 (107)	74 (136)	91 (104)	95 (106)	89 (89)
6b	87 (84)	57 (87)	**2 (32)**	45 (84)	58 (90)	90 (83)	68 (82)	76 (82)
6c	78 (87)	70 (82)	**13 (46)**	52 (85)	60 (66)	85 (92)	94 (83)	56 (91)

While a weak activity was noticed for most of the new thioxanthone derivatives, both compounds **6b** and **6c** were found surprisingly active against PIM1 at 10 μM and 1 μM. In order to clearly establish the potency of the polycyclic compounds **6b** and **6c**, their IC_{50} values of inhibition against both isoforms PIM1 and PIM2 were determined (Table 7). As noticed above, compound **6b** (0.37 μM) is a better inhibitor of PIM1 than **6c** (1.40 μM). While the values for **6c** are quite similar to those of **HM107-g**, showing a higher affinity for PIM2, those of **6b** do not show any preference for one of the isoforms. The presence of a second sulfur atom in **6b** seems to contribute to the inhibition of PIM1.

Table 7. IC_{50} values (μM) for the most promising PIM inhibitors (ADP-Glo method at 10 μM ATP).[a]

Compound	PIM1	PIM2
6b	0.37	0.46
6c	1.40	0.65
HM107-g	1.68 (0.61)[b]	0.42
SGI-1776	0.09 (0.01)[c]	0.17 (0.63)[b]

[a] A known inhibitor (**SGI-1776**) was also measured as control. [b] Value obtained previously (radioactive method at 15 μM ATP) [4]. [c] Value obtained from the literature (radioactive method) [24].

In order to have a better idea of the selectivity of the inhibitors **6b** and **6c**, they were tested on an additional panel of disease-related protein kinases: cyclin-dependent kinase 5 (CDK5/p25), proto-oncogene 1, non-receptor tyrosine kinase ABL1, tyrosine-protein kinase JAK3, serine/threonine-protein kinases Aurora B and Nek 6, glycogen-synthase kinase-3 (GSK3; isoforms α and β) and casein kinase 1 (CK1; isoform ε) (Table 8). Since competitive inhibition was only observed for JAK3 and GSK3β at 10 μM, the selectivity is rather good on this panel of 16 kinases including CLK, DYRK, GSK, CK and Haspin which can be co-inhibited by PIM1 inhibitors [25, 26] (Tables 6 and 8).

Table 8. Inhibitory activities of synthesized compounds against another panel of disease-related protein kinases. See details in Table 6. Kinases are from human origin.

Compound	CDK5/p25	ABL1	JAK3	AuroraB	Nek6	GSK3α	GSK3β	CK1ε
6b	93 (88)	63 (88)	**20** (89)	80 (≥100)	≥100 (≥100)	60 (98)	**41** (86)	62 (≥100)
6c	79 (≥100)	78 (≥100)	**18** (≥100)	93 (≥100)	≥100 (≥100)	55 (≥100)	**42** (≥100)	69 (≥100)

To help rationalize the good inhibitory activity recorded for the hexacyclic compounds, we investigated the putative binding mode of the best active compound **6b** within PIM1 ATP-binding pocket using molecular modeling experiments. However, as already observed in the corresponding ORTEP diagram (Figure 6), compound **6b** is not fully planar and tends to adopt a helicoidal chiral structure. As it is known that chiral helicenes might discriminate chiral biological targets [27, 28], and although we work in racemic series, the possible helix interconversion deserves to be looked at.

The study of the interconversion mechanism between *M* and *P* helixes [29] using Gaussian 09 [30] demonstrated a similar pathway and an energy barrier of the same order of magnitude than those observed for the [5]helicenes [29, 31, 32], showing that the interconversion of the two forms is possible (Figure 10).

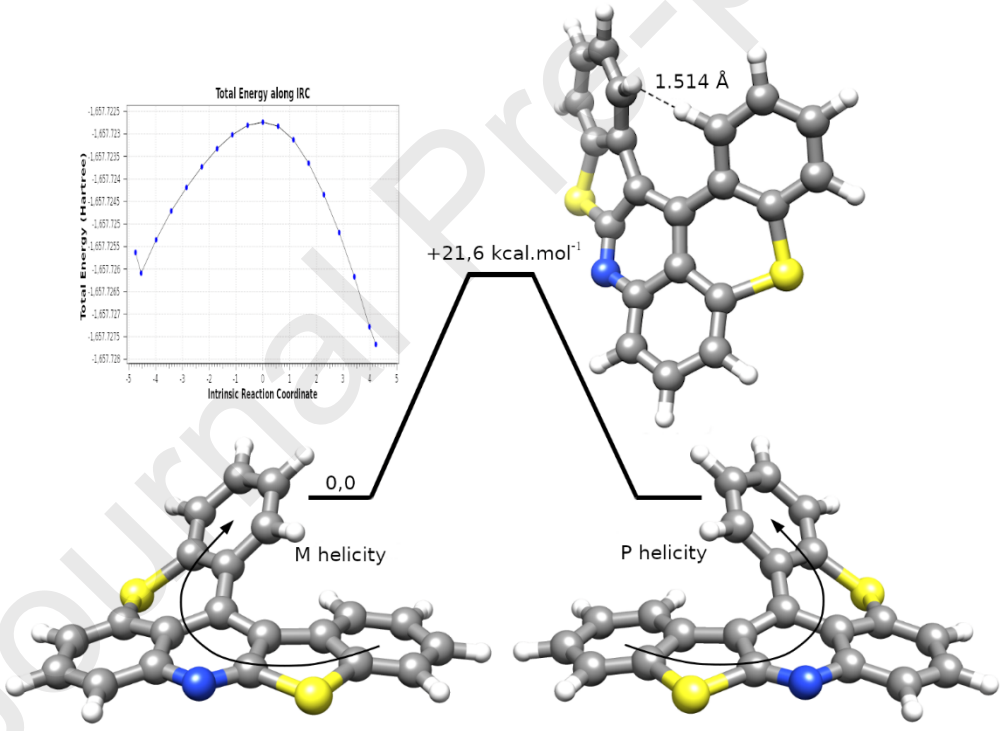

Figure 10. Isomerization pathway between *M* and *P* helixes of **6b**.

The docking studies were performed, for the two possible structures, with a PIM1 model generated from 3JPV structure available in the Protein Data Bank [33] using AutoDock Vina [34, 35]. As **6b** *M* and *P* helixes can be interconverted, only the best docking result is described. The binding mode

presented in Figure 11A depicts the interaction between PIM1 and **6b** *M* helix that, due to a better adaptation of its curvature to the ATP site, penetrates deeper inside the pocket compared with the **6b** *P* helix. After molecular dynamic analysis, the observed binding mode showed that hydrogen-bonding was established between compound **6b** and the targeted kinase via water molecules, Wat1 and Wat2. Both water molecules are commonly observed in PIM1 X-ray crystallographic structures such as 3JPV, 2C3I [36], 6NO9 [37] and 5V82 [38]. However, the hexacyclic scaffold is highly stabilized in the ATP-binding pocket via several hydrophobic interactions involving Ile104, Leu120, Val126, Leu174 and Ile185 residues as well as Leu44 and Val52 (not indicated in Figure 11A to allow a better visualization of the image).

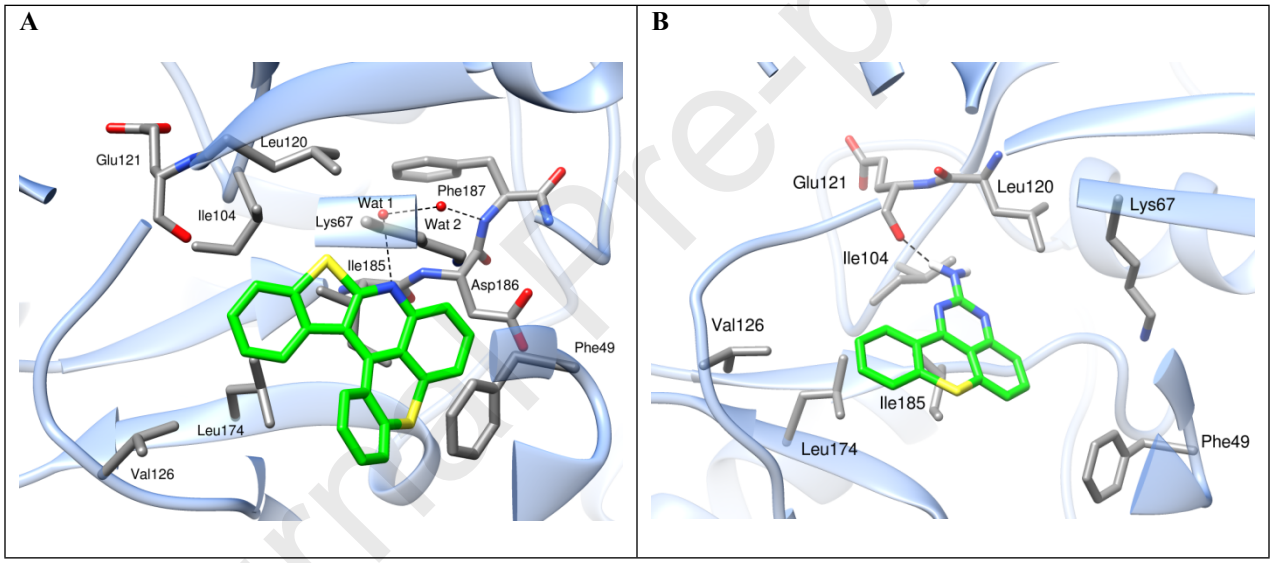

Figure 11. A) Binding mode of compound **6b** (*M* helix; **A**) and **HM107-g** (**B**) within PIM1 ATP-binding site studied by molecular modeling experiments. The images were produced using UCSF Chimera [39].

In previous studies, compound **HM107-g**, a related tetracyclic heteroaromatic was identified as well as a sub-micromolar PIM1 inhibitor [4]. Therefore, in order to compare with **6b**, the same method of molecular modeling docking experiments was used to evidence the molecular interactions established between **HM107-g** and PIM1 (Figure 11B). Compound **HM107-g** is fully planar, inserted into the

ATP-binding pocket where it is stabilized via hydrophobic interactions with the same residues as **6b**. Moreover, the amino group is H-bonded with backbone carbonyl group of Glu121 hinge region residue.

The results here reported constitute the first information related to the putative binding mode. They give us valuable information useful to optimize the biological profile of this new series of heteroaromatic compounds. For example, introduction of substituents on **6b** could allow for the formation of direct H-bonds with PIM1 binding site.

2.4. Biological evaluation on cancer cell lines

As most of our original thioxanthone derivatives were lacking biological effect on kinases, we finally evaluated their activity on cancer cell lines. Thus, the 1-(arylamino)-9-thioxanthones **2a'**, **3a**, **3b**, **3c** and **3d** were evaluated against K562 lymphoma cells, but none of them exhibited an antiproliferative activity. The compound **6b** as well as the PIM inhibitor **HM107-g** [4] were tested against HuH7 (liver), CaCo-2 and HCT116 (colon), MCF7 (breast), MDA-MB-231 and MDA-MB-468 (triple neg. breast), PC3 (prostate) cancer cell lines. In spite of the expression of PIM kinases by more than half of the selected cells (e.g. HCT166 [40], MCF7 [41], MDA-MB-231 [42] and PC3 [43]), no clear antiproliferative activity was detected after 48 h.

The compounds **6b** and **HM107-g** [4] were also evaluated against melanoma cells. Indeed, due to important mortality rate, the identification of other pharmacological targets and the development of new drugs to treat melanoma are required [44]. In addition, while PIM kinases are expressed in tumor tissue of melanoma patients, inhibitors such as **SGI-1776** limit the invasion, proliferation and viability of melanoma cells on *in vitro* models [45]. Because of their relevant mutations, the A2058 human melanoma cells are appropriate to study the antiproliferative activity of both compounds. Growth inhibitions of 38.5% ± 4.2% and 48.1% ± 2.9% were respectively induced at 10^{-5} M after 72 h by the compounds **6b** and **HM107-g**. These anti-melanoma activities are promising [46], and the rationalization of this effect will soon be studied.

3. Conclusion

Here, we have developed a short methodology to access 1-amino substituted thioxanthone derivatives, highlighting an interesting *N*-arylation-cyclization process able to deliver hexacyclic structures that would otherwise require multi-step syntheses. No biological activity was identified from the synthesized 1-(arylamino)thioxanthones. In contrast, even if these results will need to be complemented with more in-depth studies, the fluorescent [1]benzo(thio)pyrano[4,3,2-*de*]benzothieno[2,3-*b*]quinoline derivatives **6b** and **6c** already proved to inhibit the kinases PIM1 and PIM2 in a rather selective fashion; in addition, they showed promising results against melanoma cells. Therefore, in view of the modeling studies related to their putative binding mode, these results lay the ground for the rational design of a new generation of PIM-targeting fluorescent compounds.

4. Experimental

4.1. General

All reactions were performed under an argon atmosphere. THF was freshly distilled over sodium/benzophenone. The other solvents did not require any pre-treatment. Column chromatography separations were achieved on silica gel (40-63 μm). Melting points were measured on a Kofler apparatus. IR spectra were taken on a Perkin-Elmer Spectrum 100 spectrometer. ^{1}H and ^{13}C Nuclear Magnetic Resonance (NMR) spectra were recorded either on a Bruker Avance III spectrometer at 300 MHz and 75 MHz respectively, on a Bruker Avance III spectrometer at 400 MHz and 100 MHz respectively, or on a Bruker Avance III HD spectrometer at 500 MHz and 126 MHz respectively. ^{1}H chemical shifts (δ) are given in ppm relative to the solvent residual peak and ^{13}C chemical shifts are relative to the central peak of the solvent signal [47]. $ZnCl_2 \cdot$TMEDA [48], activated Cu [49], 2-iodobenzothiophene [50, 51] and 2-iodobenzofuran [50, 51] were prepared as described previously. All reagents not listed in the publication were obtained from commercial sources.

Crystallography. CCDC 1942631 (**1'**), 1942632 (**2a**), 1942633 (**2a'**), 1942634 (**2b'**), 1942635 (**3a**), 1942636 (**3c**), 1942637 (**3c'**), 1942638 (**3d**), 1942639 (**3e**), 1942640 (**3e'**), 1942641 (**5b**), 1942642 (**6b**) and 1942643 (**6c**) contain the crystallographic data for this paper. These data can be obtained free of charge from The Cambridge Crystallographic Data Centre.

The X-ray diffraction data were collected by using a D8 VENTURE Bruker AXS diffractometer equipped with a (CMOS) PHOTON 100 detector at the temperature given in the crystal data. The samples were studied with monochromatized Mo-Kα radiation (λ = 0.71073 Å, multilayer monochromator). The structure was solved by dual-space algorithm using the *SHELXT* program [52], and then refined with full-matrix least-square methods based on F^2 (*SHELXL-2014*) [53]. All non-hydrogen atoms were refined with anisotropic atomic displacement parameters. Except the nitrogen-linked hydrogen atoms that were introduced in the structural model through Fourier difference maps analysis in the case of **2a**, **2b'**, **3a**, **3c**, **3d**, **3e** and **5b**, H atoms were finally included in their calculated positions (and treated as riding on their parent atom with constrained thermal parameters in the case of **2a**, **2a'**, **2b'**, **3d**, **3e**, **3e'** and **6b**). The molecular diagrams were generated by ORTEP-3 (version 2.02) [54].

4.2. 1-Iodo-9-thioxanthone (1). To a stirred mixture of 9-thioxanthone (0.20 g, 1.0 mmol) and $ZnCl_2$·TMEDA (0.26 g, 1.0 mmol) in THF (3 mL) at -30 °C was added dropwise a solution of LiTMP (prepared by adding BuLi (about 1.6 M hexanes solution, 1.5 mmol) to a stirred, cooled (0 °C) solution of 2,2,6,6-tetramethylpiperidine (0.25 mL, 1.5 mmol) in THF (3 mL) and stirring for 5 min) cooled at -30 °C. After 15 min at -30 °C, a solution of I_2 (0.38 g, 1.5 mmol) in THF (5 mL) was introduced, and the mixture was stirred overnight before addition of an aqueous saturated solution of $Na_2S_2O_3$ (5 mL) and extraction with AcOEt (3 x 20 mL). The combined organic layers were dried over $MgSO_4$, filtered and concentrated under reduced pressure. The crude product was purified by chromatography over silica gel (eluent: heptane-AcOEt 80:20). Compound **1** was isolated in 84% yield as a yellow powder:

mp 152 °C; ^{1}H NMR ($CDCl_3$) δ 7.10 (t, 1H, *J* = 7.8 Hz), 7.41-7.47 (m, 2H), 7.52-7.60 (m, 2H), 8.14 (dd, 1H, *J* = 7.5 and 1.2 Hz), 8.47 (dm, 1H, *J* = 8.1 Hz); ^{13}C NMR ($CDCl_3$) δ 94.8 (C), 125.5 (CH), 126.7 (CH), 126.8 (CH), 127.7 (C), 129.6 (C), 130.2 (CH), 131.8 (CH), 132.3 (CH), 135.0 (C), 138.7 (C), 141.8 (CH), 179.5 (C). The analyses are as described previously [12]. **1,8-Diiodo-9-thioxanthone (1')** was also isolated in 10% yield as a white powder: mp 162 °C; IR (ATR): 674, 725, 760, 776, 791, 894, 919, 1060, 1080, 1162, 1205, 1278, 1423, 1545, 1567, 1654, 2852, 2922, 3048 cm^{-1}; ^{1}H NMR ($CDCl_3$) δ 7.11 (t, 2H, *J* = 7.9 Hz), 7.51 (dd, 2H, *J* = 8.0 and 1.1 Hz), 8.05 (dd, 2H, *J* = 7.7 and 1.1 Hz); ^{13}C NMR ($CDCl_3$) δ 94.5 (2C), 125.9 (2CH), 131.5 (2CH), 132.0 (2C), 136.3 (2C), 140.7 (2CH), 183.7 (C). **Crystal data for 1'.** $C_{13}H_6I_2OS$, *M* = 464.04, *T* = 150(2) K, triclinic, *P* -1, *a* = 7.5979(14), *b* = 11.307(2), *c* = 16.538(3) Å, α = 75.648(7), β = 73.865(6), γ = 72.133(6) °, *V* = 1278.3(4) Å^3, *Z* = 4, *d* = 2.411 g.cm^{-3}, μ = 5.062 mm^{-1}. A final refinement on F^2 with 5588 unique intensities and 308 parameters converged at ω$R(F^2)$ = 0.1077 ($R(F)$ = 0.0509) for 4445 observed reflections with $I > 2\sigma(I)$. CCDC 1942631.

4.3. *N*-Arylation of aromatic diamines by 1-iodo-9-thioxanthone (1)

4.3.1. General procedure 1: A degassed mixture of the required aromatic diamine (2.0 mmol), 1-iodo-9-thioxanthone (**1**; 0.34 g, 1.0 mmol), CuI (37 mg, 0.2 mmol), K_2CO_3 (0.14 g, 1.0 mmol) and DMSO (1 mL) was heated at 120 °C overnight. After cooling to room temperature, aqueous 25% NH_4OH (5 mL) was added. Extraction using AcOEt (3x20 mL), removal of the solvent and purification by chromatography on silica gel (the eluent is given in the product description) led to the expected compound.

4.3.2. 1-(2-Aminophenylamino)-8-thioxanthone (2a'). The general procedure 1 was applied to 1,2-phenylenediamine (0.22 g) to afford the compound **2a'** (eluent: heptane-AcOEt 90:10) in 58% yield as an orange powder: mp 184-185 °C; IR (ATR): 670, 718, 735, 769, 1081, 1155, 1183, 1227, 1267, 1307, 1381, 1435, 1463, 1491, 1513, 1556, 1568, 1590, 3360, 3443 cm^{-1}; ^{1}H NMR ($CDCl_3$) δ 3.85 (br s, 2H),

6.54 (dd, 1H, *J* = 8.5 and 1.1 Hz), 6.80 (td, 2H, *J* = 7.9 and 1.2 Hz), 6.85 (dd, 1H, *J* = 8.0 and 1.4 Hz), 7.12 (td, 1H, *J* = 7.7 and 1.5 Hz), 7.20 (dd, 1H, *J* = 7.8 and 1.5 Hz), 7.25 (t, 1H, *J* = 8.0 Hz), 7.43 (ddd, 1H, *J* = 8.2, 7.0 and 1.3 Hz), 7.48 (dd, 1H, *J* = 8.0 and 1.2 Hz), 7.56 (ddd, 1H, *J* = 8.3, 7.0 and 1.5 Hz), 8.55 (dd, 1H, *J* = 8.2 and 1.4 Hz), 11.35 (br s, 1H); ^{13}C NMR ($CDCl_3$) δ 110.1 (CH), 113.2 (CH), 113.5 (C), 116.2 (CH), 119.0 (CH), 125.3 (CH), 125.6 (C), 126.1 (CH), 127.6 (CH), 128.1 (CH), 129.6 (CH), 130.5 (C), 132.1 (CH), 133.6 (CH), 136.7 (C), 139.5 (C), 143.3 (C), 152.6 (C), 183.8 (C). **Crystal data for 2a'.** $C_{19}H_{14}N_2OS$, *M* = 318.38, *T* = 150(2) K, triclinic, *P* -1, *a* = 3.9485(10), *b* = 13.778(3), *c* = 27.364(7) Å, α = 78.249(8), β = 90.887(10), γ = 81.795(10) °, *V* = 1441.0(6) Å^3, *Z* = 4, *d* = 1.468 g.cm^{-3}, μ = 0.231 mm^{-1}. A final refinement on F^2 with 6530 unique intensities and 331 parameters converged at ω$R(F^2)$ = 0.4732 ($R(F)$ = 0.1994) for 4965 observed reflections with $I > 2\sigma(I)$. CCDC 1942633. Traces of **2a** also formed in the same reaction, as identified by X-ray diffraction. **Crystal data for 2a.** $C_{19}H_{12}N_2S$, *M* = 300.37, *T* = 150(2) K, orthorhombic, *P b c a*, *a* = 16.0429(8), *b* = 8.0742(4), *c* = 21.7145(9) Å, *V* = 2812.8(2) Å^3, *Z* = 8, *d* = 1.419 g.cm^{-3}, μ = 0.227 mm^{-1}. A final refinement on F^2 with 3229 unique intensities and 202 parameters converged at ω$R(F^2)$ = 0.0921 ($R(F)$ = 0.0373) for 2761 observed reflections with $I > 2\sigma(I)$. CCDC 1942632.

4.3.3. 1-(3-Amino-2-pyridylamino)-9-thioxanthone (2b'). The general procedure 1 was applied to 2,3-diaminopyridine (0.22 g) to afford the compound **2b'** (eluent: heptane-AcOEt 70:30) in 35% yield as an orange powder: mp 196 °C; IR (ATR): 668, 715, 743, 768, 922, 1083, 1156, 1185, 1231, 1271, 1306, 1431, 1516, 1574, 1630, 2925 cm^{-1}; ^{1}H NMR ($CDCl_3$) δ 3.91 (br s, 2H), 6.85 (dd, 1H, *J* = 7.7 and 4.8 Hz), 7.02 (dd, 1H, *J* = 7.9 and 1.1 Hz), 7.08 (dd, 1H, *J* = 7.8 and 1.6 Hz), 7.44 (ddd, 1H, *J* = 8.2, 6.9 and 1.2 Hz), 7.47-7.51 (m, 2H), 7.58 (ddd, 1H, *J* = 8.2, 7.0 and 1.5 Hz), 7.90 (dd, 1H, *J* = 4.8 and 1.6 Hz), 8.50 (dd, 1H, *J* = 8.4 and 1.45 Hz), 8.59 (dd, 1H, *J* = 8.1 and 1.4 Hz), 12.66 (br s, 1H); ^{13}C NMR ($CDCl_3$) δ 113.9 (CH), 114.8 (C), 115.8 (CH), 118.4 (CH), 122.7 (CH), 125.3 (CH), 126.2 (CH), 129.9 (CH), 130.4 (C), 132.2 (CH), 133.0 (C), 133.7 (CH), 136.9 (C), 137.8 (CH), 139.3 (C), 143.7 (C), 148.4 (C), 184.1 (C). **Crystal data for 2b'.** $C_{18}H_{13}N_3OS$, *M* = 319.37, *T* = 150(2) K, monoclinic,

$P\,2_1/c$, a = 13.8914(13), b = 5.2102(4), c = 19.8060(18) Å, β = 90.209(4) °, V = 1433.5(2) Å^3, Z = 4, d = 1.480 g.cm^{-3}, μ = 0.234 mm^{-1}. A final refinement on F^2 with 3276 unique intensities and 217 parameters converged at ωR(F^2) = 0.0955 (R(F) = 0.0490) for 2256 observed reflections with $I > 2\sigma(I)$. CCDC 1942634.

4.4. *N*-Arylation of anilines by 1-iodo-9-thioxanthone (1)

4.4.1. General procedure 2: A degassed mixture of the required aniline (1.0 mmol), 1-iodo-9-thioxanthone (**1**; 0.34 g, 1.0 mmol), CuI (28 mg, 0.15 mmol), K_2CO_3 (0.28 g, 2.0 mmol) and DMSO (0.5 mL) was heated at 120 °C for 24 h. The purification procedure is given in the product description.

4.4.2. 1-(4-(Trifluoromethylsulfonyl)phenylamino)-9-thioxanthone (3a). The general procedure 2 was applied to 4-[(trifluoromethyl)sulfonyl]aniline (0.23 g). After cooling to room temperature, water (5 mL) was added and the crude product was filtrated. Purification of the solid by chromatography on silica gel (eluent: heptane-AcOEt 80:20) led to the expected compound **3a** in 58% yield as a yellow powder: mp 175 °C; IR (ATR): 666, 676, 704, 748, 756, 776, 1071, 1138, 1178, 1201, 1289, 1357, 1436, 1511, 1556, 1568, 3060 cm^{-1}; ^{1}H NMR ($CDCl_3$) δ 7.15 (dd, 1H, J = 6.6 and 2.4 Hz), 7.45-7.55 (m, 6H), 7.63 (ddd, 1H, J = 8.3, 6.9 and 1.5 Hz), 7.92-7.95 (m, 2H), 8.52 (ddd, 1H, J = 8.1, 1.5 and 0.6 Hz), 12.27 (br s, 1H); ^{13}C NMR ($CDCl_3$) δ 113.1 (CH), 116.5 (C), 118.2 (CH), 119.1 (2CH), 121.9 (C), 125.4 (CH), 126.7 (CH), 129.8 (CH), 130.2 (C), 132.7 (CH), 133.0 (2CH), 133.1 (CH), 136.6 (C), 140.5 (C), 146.6 (C), 149.4 (C), 184.0 (C), CF_3 not seen. **Crystal data for 3a.** $C_{20}H_{12}F_3NO_3S_2$, M = 435.43, T = 150(2) K, triclinic, P -1, a = 7.2523(12), b = 7.9427(13), c = 16.411(3) Å, α = 98.518(6), β = 100.915(6), γ = 101.305(6) °, V = 893.2(3) Å^3, Z = 2, d = 1.619 g.cm^{-3}, μ = 0.352 mm^{-1}. A final refinement on F^2 with 4054 unique intensities and 140 parameters converged at ωR(F^2) = 0.3297 (R(F) = 0.1093) for 3779 observed reflections with $I > 2\sigma(I)$. CCDC 1942635.

4.4.3. 1-(4-Fluorophenylamino)-9-thioxanthone (3b). The general procedure 2 was applied to 4-fluoroaniline (95 µL). After cooling to room temperature, an aqueous saturated solution of NH_4Cl (5 mL) was added and the product was extracted by using AcOEt (3x20 mL). Drying over Na_2SO_4,

removal of the solvent and purification by chromatography on silica gel (eluent: heptane-AcOEt 75:25) led to the expected compound **3b** in 31% yield as a yellow powder: mp 114 °C; IR (ATR): 669, 744, 759, 826, 1151, 1180, 1210, 1267, 1437, 1512, 1560, 1578, 3060 cm^{-1}; ^1H NMR ($CDCl_3$) δ 6.85 (dd, 1H, *J* = 7.7 and 1.1 Hz), 6.94 (dd, 1H, *J* = 8.5 and 1.1 Hz), 7.05-7.13 (m, 2H), 7.24-7.32 (m, 3H), 7.45 (ddd, 1H, *J* = 8.3, 6.9 and 1.4 Hz), 7.46-7.49 (m, 1H), 7.59 (ddd, 1H, *J* = 8.3, 6.9 and 1.5 Hz), 8.55 (ddd, 1H, *J* = 8.1, 1.5 and 0.6 Hz), 11.75 (br s, 1H); ^{13}C NMR ($CDCl_3$) δ 109.6 (CH), 113.5 (CH), 113.6 (C), 116.4 (d, 2CH, *J* = 22.4 Hz), 125.2 (CH), 126.2 (CH), 126.4 (d, 2CH, *J* = 8.1 Hz), 129.6 (CH), 130.4 (C), 132.1 (CH), 133.4 (CH), 136.3 (C), 136.7 (C), 139.7 (C), 152.0 (C), 160.1 (d, C, *J* = 244 Hz), 183.7 (C). Anal. Calcd for $C_{19}H_{12}FNOS$ (321.37): C, 71.01; H, 3.76; N, 4.36. Found: C, 71.14; H, 3.95; N, 4.29.

4.4.4. 1-(4-Tolylamino)-9-thioxanthone (3c). The general procedure 2 was applied to 4-toluidine (0.11 g). After cooling to room temperature, an aqueous saturated solution of NH_4Cl (5 mL) was added and the product was extracted by using AcOEt (3x20 mL). Drying over Na_2SO_4, removal of the solvent and purification by chromatography on silica gel (eluent: heptane-AcOEt-Et_3N 80:15:5) led to a mixture from which the expected compound **3c** (estimated yield from a mixture with **3c'**: 50% yield) was identified by NMR and crystal data. ^1H NMR ($CDCl_3$, selected data) δ 1.54 (s, 3H), 6.80 (dd, 1H, *J* = 7.7 and 1.1 Hz), 7.02 (dd, 1H, *J* = 8.5 and 1.1 Hz), 8.52 (dd, 1H, *J* = 8.1 and 1.2 Hz), 11.75 (br s, 1H). **Crystal data for 3c.** $C_{20}H_{15}NOS$, *M* = 317.39, *T* = 150(2) K, monoclinic, *P* $2_1/c$, *a* = 12.8049(11), *b* = 12.0640(10), *c* = 10.7591(8) Å, β = 114.737(3) °, *V* = 1509.5(2) $Å^3$, *Z* = 4, *d* = 1.397 $g.cm^{-3}$, μ = 0.218 mm^{-1}. A final refinement on F^2 with 3443 unique intensities and 212 parameters converged at $\omega R(F^2)$ = 0.0944 ($R(F)$ = 0.0360) for 2849 observed reflections with $I > 2\sigma(I)$. CCDC 1942636. The compound **3c'** was also isolated in 6% yield as a red powder: mp 221 °C; IR (ATR): 670, 717, 741, 754, 767, 1184, 1229, 1268, 1436, 1497, 1513, 1558, 1568, 1608, 3051 cm^{-1}; ^1H NMR ($CDCl_3$) δ 2.30 (s, 3H), 7.05-7.19 (m, 12H), 7.28 (ddd, 2H, *J* = 8.9, 7.3 and 1.6 Hz), 7.36 (ddd, 2H, *J* = 7.8, 1.6, 0.6 Hz), 7.45 (t, 2H, *J* = 8.0 Hz); ^{13}C NMR ($CDCl_3$) δ 21.1 (CH_3), 119.9 (2CH), 121.8 (2C), 124.5 (2CH),

124.8 (2CH), 126.1 (2CH), 126.6 (2CH), 128.1 (2CH), 130.0 (2CH), 130.9 (2CH), 132.4 (2CH), 132.6 (2C), 133.8 (C), 134.9 (2C), 138.4 (2C), 145.8 (C), 150.0 (2C), 181.9 (2C). **Crystal data for 3c'.** $C_{33}H_{21}NO_2S_2$, M = 527.63, T = 150(2) K, monoclinic, $P\,2_1/c$, a = 18.500(3), b = 9.1189(18), c = 15.199(2) Å, β = 95.212(6) °, V = 2553.4(8) Å^3, Z = 4, d = 1.373 g.cm^{-3}, μ = 0.241 mm^{-1}. A final refinement on F^2 with 5824 unique intensities and 344 parameters converged at ωR(F^2) = 0.0952 (R(F) = 0.0406) for 4756 observed reflections with $I > 2\sigma(I)$. CCDC 1942637.

4.4.5. 1-(α-Naphthylamino)-9-thioxanthone (3d). The general procedure 2 was applied to α-naphthylamine (0.14 g). After cooling to room temperature, an aqueous saturated solution of NH_4Cl (5 mL) was added and the product was extracted by using AcOEt (3x20 mL). Drying over Na_2SO_4, removal of the solvent and purification by chromatography on silica gel (eluent: heptane-AcOEt 85:15) led to the expected compound **3d** in 63% yield as an orange powder: mp 198 °C; IR (ATR): 670, 717, 742, 755, 767, 1082, 1154, 1184, 1229, 1268, 1376, 1436, 1497, 1514, 1558, 1569, 1592, 1608, 3050 cm^{-1}; ^{1}H NMR ($CDCl_3$) δ 6.76 (dd, 1H, J = 8.5 and 1.1 Hz), 6.82 (dd, 1H, J = 7.7 and 1.1 Hz), 7.20 (t, 1H, J = 8.1 Hz), 7.45 (ddd, 1H, J = 8.2, 7.0 and 1.3 Hz), 7.42-7.61 (m, 6H), 7.76 (d, 1H, J = 8.2 Hz), 7.88-7.93 (m, 1H), 8.15 (dt, 1H, J = 8.1 and 1.0 Hz), 8.59 (ddd, 1H, J = 8.2, 1.5 and 0.6 Hz), 12.2 (br s, 1H); ^{13}C NMR ($CDCl_3$) δ 110.5 (CH), 113.3 (CH), 113.6 (C), 122.3 (CH), 123.2 (CH), 125.2 (CH), 126.0 (CH), 126.0 (CH), 126.1 (CH), 126.5 (CH), 126.5 (CH), 128.5 (CH), 129.7 (CH), 130.1 (C), 130.5 (C), 132.1 (CH), 133.4 (CH), 135.0 (C), 136.5 (C), 136.8 (C), 139.5 (C), 152.9 (C), 183.9 (C). **Crystal data for 3d.** $C_{23}H_{15}NOS$, M = 353.42, T = 150(2) K, monoclinic, $P\,2_1/c$, a = 25.757(6), b = 3.8988(10), c = 15.909(4) Å, β = 90.430(7) °, V = 1597.5(7) Å^3, Z = 4, d = 1.469 g.cm^{-3}, μ = 0.215 mm^{-1}. A final refinement on F^2 with 3616 unique intensities and 238 parameters converged at ωR(F^2) = 0.1196 (R(F) = 0.0590) for 2517 observed reflections with $I > 2\sigma(I)$. CCDC 1942638.

4.4.6. 1-(4-Methoxyphenylamino)-9-thioxanthone (3e). The general procedure 2, but with only 0.5 mmol of the required aniline, was applied to 4-anisidine (62 mg). After cooling to room temperature, an aqueous saturated solution of NH_4Cl (5 mL) was added and the products were extracted by using

AcOEt (3x20 mL). Drying over Na_2SO_4, removal of the solvent and purification by chromatography on silica gel (eluent: heptane-CH_2Cl_2 80:20) led to a mixture from which the compound **3e** (estimated yield < 10% yield) was identified by NMR and crystal data. ^{1}H NMR ($CDCl_3$) δ 3.84 (s, 3H), 6.77 (dd, 1H, *J* = 7.7 and 1.1 Hz), 6.86 (dd, 1H, *J* = 8.5 and 1.1 Hz), 6.92-6.97 (m, 2H), 7.20-7.27 (m, 3H), 7.42 (ddd, 1H, *J* = 8.3, 6.9 and 1.4 Hz), 7.44-7.48 (m, 1H), 7.55 (ddd, 1H, *J* = 8.3, 6.9 and 1.5 Hz), 8.52 (ddd, 1H, *J* = 8.1, 1.5 and 0.6 Hz), 11.65 (br s, 1H). **Crystal data for 3e.** $C_{20}H_{15}NO_2S$, *M* = 333.39, *T* = 150(2) K, triclinic, *P* -1, *a* = 7.7122(7), *b* = 8.5030(7), *c* = 12.1561(10) Å, α = 80.111(3), β = 79.888(4), γ = 82.854(3) °, *V* = 769.46(11) Å^3, *Z* = 2, *d* = 1.439 g.cm^{-3}, μ = 0.222 mm^{-1}. A final refinement on F^2 with 3499 unique intensities and 221 parameters converged at ω$R(F^2)$ = 0.1269 ($R(F)$ = 0.0491) for 2897 observed reflections with $I > 2\sigma(I)$. CCDC 1942639. The compound **3e'** was isolated in 41% yield as a red powder: mp 194 °C; IR (ATR): 682, 727, 749, 770, 783, 832, 915, 1026, 1176, 1242, 1261, 1277, 1435, 1504, 1570, 1642, 2965 cm^{-1}; ^{1}H NMR ($CDCl_3$) δ 3.79 (s, 3H), 6.80-6.85 (m, 2H), 7.06 (d, 2H, *J* = 7.9 Hz), 7.09-7.17 (m, 8H), 7.16-7.21 (m, 2H), 7.33 (d, 2H, *J* = 9.0 Hz), 7.44 (t, 2H, *J* = 8.0 Hz); ^{13}C NMR ($CDCl_3$) δ 55.7 (CH_3), 114.9 (CH), 119.5 (CH), 121.1 (C), 124.4 (CH), 126.1 (CH), 126.1 (CH), 127.0 (CH), 128.0 (CH), 130.9 (CH), 132.4 (CH), 132.6 (C), 134.8 (C), 138.4 (C), 141.3 (C), 150.3 (C), 156.9 (C), 182.0 (C). **Crystal data for 3e'.** $C_{33}H_{21}NO_3S_2$, *M* = 543.63, *T* = 150(2) K, monoclinic, *P* $2_1/n$, *a* = 15.0958(5), *b* = 9.4474(4), *c* = 18.1199(6) Å, β = 103.5890(10) °, *V* = 2511.85(16) Å^3, *Z* = 4, *d* = 1.438 g.cm^{-3}, μ = 0.251 mm^{-1}. A final refinement on F^2 with 5710 unique intensities and 353 parameters converged at ω$R(F^2)$ = 0.0905 ($R(F)$ = 0.0408) for 4390 observed reflections with $I > 2\sigma(I)$. CCDC 1942640.

4.4.7. 1-(4-Pyridylamino)-9-thioxanthone. A mixture of 4-aminopyridine (94 mg, 1.0 mmol), 1-iodo-9-thioxanthone (**1**; 0.40 g, 1.2 mmol), Cu (11 mg, 0.16 mmol), CuI (11 mg, 0.06 mmol), K_2CO_3 (0.28 g, 2.0 mmol) and DMF (0.5 mL) was heated at 140 °C for 6 h. After cooling to room temperature, water (5 mL) was added and the crude product was filtrated. Purification of the solid by chromatography on silica gel (eluent: CH_2Cl_2-heptane 40:60 to 100:00) led to **3f** in 49% yield as a

yellow powder: mp 150 °C; IR (ATR): 715, 747, 772, 814, 909, 961, 1079, 1159, 1182, 1277, 1310, 1444, 1515, 1557, 1576, 1734, 2855, 2924, 2955 cm^{-1}; ^1H NMR ($CDCl_3$) δ 7.09 (dd, 1H, *J* = 7.1 and 1.9 Hz), 7.21-7.23 (m, 2H), 7.42-7.53 (m, 4H), 7.60 (ddd, 1H, *J* = 8.3, 6.9 and 1.5 Hz), 8.45-8.47 (m, 2H), 8.52 (ddd, 1H, *J* = 8.1, 1.5 and 0.6 Hz), 12.03 (br s, 1H); ^{13}C NMR ($CDCl_3$) δ 113.0 (CH), 113.8 (CH), 116.2 (C), 117.5 (CH), 125.4 (2CH), 126.6 (CH), 129.8 (CH), 130.3 (C), 132.6 (CH), 133.1 (CH), 136.6 (C), 140.3 (C), 147.0 (C), 148.9 (C), 150.1 (2CH), 183.9 (C). Anal. Calcd for $C_{18}H_{12}N_2OS$ (304.37): C, 71.03; H, 3.97; N, 9.20. Found: C, 71.37; H, 4.29; N, 8.94.

4.5. 1-Amino-9-thioxanthone (4) [55] was prepared by slightly modifying a literature procedure [19]. A degassed (argon) mixture of 1-iodo-9-thioxanthone (**1**; 0.51 g, 1.5 mmol), CuI (29 mg, 0.15 mmol), DMEDA (24 µL, 0.22 mmol) and DMSO (0.75 mL) was treated by 25% NH_4OH (2.3 mL) and the mixture was heated in a sealed tube at 130 °C for 16 h. After cooling to room temperature, brine (10 mL) was added before extraction using AcOEt (3x20 mL), removal of the solvent and purification by chromatography on silica gel (eluent: heptane-AcOEt 85:15). Compound **4** was isolated in 50% yield as a yellow powder: mp 145 °C; ^1H NMR ($CDCl_3$) δ 6.56 (dd, 1H, *J* = 8.2 and 1.1 Hz), 6.76 (dd, 1H, *J* = 7.7 and 1.1 Hz), 6.99 (br s, 2H), 7.25 (t, 1H, *J* = 8.0 Hz), 7.40 (ddd, 1H, *J* = 8.3, 6.9 and 1.4 Hz), 7.42-7.46 (m, 1H), 7.53 (ddd, 1H, *J* = 8.3, 6.9 and 1.5 Hz), 8.50 (ddd, 1H, *J* = 8.0, 1.5 and 0.6 Hz); ^{13}C NMR ($CDCl_3$) δ 113.0 (CH), 113.2 (CH), 113.4 (C), 125.3 (CH), 126.0 (CH), 129.6 (CH), 130.5 (C), 132.0 (CH), 133.3 (CH), 136.7 (C), 139.1 (C), 153.4 (C), 183.4 (C).

4.6. *N*-arylation of 1-amino-9-thioxanthone (4)

4.6.1. General procedure 3: The *N*-arylated substrates were prepared by slightly modifying a literature procedure [56]. To 1-amino-9-thioxanthone (**4**; 0.34 g, 1.5 mmol) and the required iodide (2.2 mmol) in Bu_2O (2 mL) were successively added activated Cu (19 mg, 0.30 mmol) and K_2CO_3 (0.43 g, 3.0 mmol). The mixture was degassed and refluxed under argon for 24 h. After cooling to room

temperature, the mixture was concentrated. Purification by chromatography on silica gel (the eluent is given in the product description) led to the expected compound.

4.6.2. 1-(2-Thienylamino)-9-thioxanthone (5a). The general procedure 3 (reaction time: 24 h) using 2-iodothiophene (0.24 mL) gave **5a** (eluent: heptane-AcOEt 80:20) in 40% yield as an orange powder: mp 160 °C; IR (ATR): 747, 1160, 1180, 1194, 1230, 1248, 1284, 1440, 1459, 1478, 1592, 1729, 2925, 3057, 3462 cm^{-1}; ^1H NMR ($CDCl_3$) δ 6.86-6.90 (m, 2H), 6.97 (dd, 1H, *J* = 5.7 and 3.7 Hz), 7.01 (dd, 1H, *J* = 8.5 and 1.1 Hz), 7.09 (dd, 1H, *J* = 5.5 and 1.4 Hz), 7.32 (ddd, 1H, *J* = 8.3, 7.7 and 0.5 Hz), 7.44 (ddd, 1H, *J* = 8.3, 6.9 and 1.4 Hz), 7.46-7.50 (m, 1H), 7.57 (ddd, 1H, *J* = 8.3, 6.9 and 1.5 Hz), 8.54 (ddd, 1H, *J* = 8.1, 1.5, 0.6 Hz), 11.75 (s, 1H); ^{13}C NMR ($CDCl_3$) δ 110.3 (CH), 113.7 (C), 114.2 (CH), 121.4 (CH), 122.0 (CH), 125.3 (CH), 126.2 (CH), 126.2 (CH), 129.7 (CH), 130.3 (C), 132.2 (CH), 133.6 (CH), 136.8 (C), 139.5 (C), 143.3 (C), 152.9 (C), 183.8 (C). Anal. Calcd for $C_{17}H_{11}NOS_2$ (309.40): C, 65.99; H, 3.58; N, 4.53. Found: C, 66.14; H, 3.51; N, 4.36.

4.6.3. 1-(2-Benzothienylamino)-9-thioxanthone (5b). The general procedure 3 using 2-iodobenzothiophene (0.57 g) gave **5b** (eluent: heptane) in 50% yield as an orange powder: mp 148 °C; IR (ATR): 670, 715, 745, 774, 1084, 1143, 1268, 1436, 1477, 1538, 1558, 1589, 1604, 3054 cm^{-1}; ^1H NMR ($CDCl_3$) δ 6.95 (dd, 1H, *J* = 7.5 and 1.4 Hz), 7.11 (s, 1H), 7.28-7.38 (m, 3H), 7.38 (t, 1H, *J* = 7.4 Hz), 7.46 (ddd, 1H, *J* = 8.3, 6.9 and 1.4 Hz), 7.48-7.52 (m, 1H), 7.59 (ddd, 1H, *J* = 8.3, 6.9 and 1.5 Hz), 7.66-7.69 (m, 1H), 7.74-7.76 (m, 1H), 8.56 (ddd, 1H, *J* = 8.1, 1.5 and 0.6 Hz), 12.16 (s, 1H); ^{13}C NMR ($CDCl_3$) δ 110.8 (CH), 114.0 (C), 115.0 (CH), 115.6 (CH), 122.3 (CH), 122.9 (CH), 123.9 (CH), 124.6 (CH), 125.3 (CH), 126.3 (CH), 129.7 (CH), 130.2 (C), 132.3 (CH), 133.5 (CH), 136.4 (C), 136.7 (C), 139.0 (C), 139.7 (C), 143.5 (C), 151.2 (C), 183.7 (C). **Crystal data for 5b.** $C_{21}H_{13}NOS_2$, *M* = 359.44, *T* = 150(2) K, monoclinic, *P* $2_1/c$, *a* = 14.1321(8), *b* = 15.6356(8), *c* = 7.3904(4) Å, β = 90.285(2) °, *V* = 1632.99(15) $Å^3$, *Z* = 4, *d* = 1.462 $g.cm^{-3}$, μ = 0.335 mm^{-1}. A final refinement on F^2 with 3686 unique intensities and 230 parameters converged at $\omega R(F^2)$ = 0.1252 ($R(F)$ = 0.0513) for 2883 observed reflections with $I > 2\sigma(I)$. CCDC 1942641.

4.6.4. [1]Benzothiopyrano[4,3,2-*de*]benzothieno[2,3-*b*]quinoline (6b). The general procedure 3 using 2-iodobenzothiophene (0.57 g) gave **6b** (eluent: heptane-AcOEt 80:20) in 38% yield as a yellow powder: mp 176 °C; IR (ATR): 690, 728, 752, 784, 812, 1064, 1111, 1147, 1160, 1199, 1309, 1354, 1473, 1537 cm^{-1}; ^1H NMR ($CDCl_3$) δ 7.22-7.25 (m, 2H), 7.40-7.46 (m, 3H), 7.54 (dd, 1H, J = 7.9 and 1.3 Hz), 7.60 (dd, 1H, J = 8.4 and 7.3 Hz), 7.82 (ddd, 1H, J = 7.9, 1.2 and 0.6 Hz), 7.85 (dd, 1H, J = 8.5, 1.1 Hz), 8.19 (dd, 1H, J = 8.0 and 1.3 Hz), 8.23 (dd, 1H, J = 8.2 and 1.0 Hz); ^{13}C NMR ($CDCl_3$) δ 120.2 (CH), 123.3 (CH), 123.4 (C), 123.7 (C), 124.0 (CH), 124.3 (CH), 125.4 (CH), 126.3 (CH), 128.0 (CH), 128.2 (CH), 129.0 (C), 129.1 (CH), 130.0 (C), 130.5 (CH), 131.0 (CH), 133.3 (C), 135.8 (C), 137.6 (C), 138.6 (C), 147.9 (C), 165.9 (C). **Crystal data for 6b.** $C_{21}H_{11}NS_2$, M = 341.43, T = 150(2) K, orthorhombic, P b c a, a = 18.151(3), b = 7.8809(10), c = 21.117(2) Å, V = 3020.8(7) $Å^3$, Z = 8, d = 1.501 $g.cm^{-3}$, μ = 0.353 mm^{-1}. A final refinement on F^2 with 3461 unique intensities and 217 parameters converged at $\omega R(F^2)$ = 0.1366 ($R(F)$ = 0.0610) for 2353 observed reflections with $I > 2\sigma(I)$. CCDC 1942642.

4.6.5. [1]Benzothiopyrano[4,3,2-*de*]benzofuro[2,3-*b*]quinoline (6c). The general procedure 3 using 2-iodobenzofuran (0.54 g) gave **6c** after removal of the solvent and purification by chromatography on silica gel (eluent: heptane-CH_2Cl_2 95:5) in 21% yield as an orange powder: mp 184 °C; IR (ATR): 671, 717, 730, 747, 894, 977, 1033, 1079, 1160, 1194, 1228, 1282, 1308, 1325, 1436, 1458, 1562, 1591, 2924, 3054, 3306, 3429 cm^{-1}; ^1H NMR ($CDCl_3$) δ 7.31 (ddd, 1H, J = 8.3, 7.4 and 1.2 Hz), 7.36-7.61 (m, 6H), 7.64 (d, 1H, J = 7.8 Hz), 7.85 (dd, 1H, J = 8.4 and 1.2 Hz), 8.22 (d, 1H, J = 7.9 Hz), 8.43 (dd, 1H, J = 7.4 and 1.6 Hz); ^{13}C NMR ($CDCl_3$) δ 112.0 (C), 112.2 (CH), 119.7 (CH), 122.8 (C), 123.0 (CH), 123.6 (C), 123.7 (CH), 124.8 (CH), 126.4 (CH), 127.3 (CH), 128.8 (C), 129.2 (CH), 129.3 (CH), 129.8 (CH), 130.3 (C), 130.7 (CH), 135.7 (C), 138.3 (C), 147.3 (C), 156.0 (C), 164.3 (C). **Crystal data for 6c.** $C_{21}H_{11}NOS$, M = 325.37, T = 150(2) K, orthorhombic, $P\,2_1\,2_1\,2_1$, a = 7.5722(4), b = 18.9340(13), c = 20.5024(14) Å, V = 2939.5(3) $Å^3$, Z = 8, d = 1.470 $g.cm^{-3}$, μ = 0.227 mm^{-1}. A final

refinement on F^2 with 6761 unique intensities and 434 parameters converged at $\omega R(F^2) = 0.1035$ ($R(F) = 0.0513$) for 5265 observed reflections with $I > 2\sigma(I)$. CCDC 1942643.

4.7. Physicochemical measurements

Measurements have been performed on freshly-prepared air-equilibrated solutions at room temperature (25 °C). UV-Vis absorption spectra were recorded on a Jasco V-570 spectrophotometer. Steady-state and time-resolved fluorescence measurements were performed in dilute solutions contained in quartz cells of 1 cm pathlength using an Edinburgh Instrument (FLS920) fluorimeter equipped with a 450 W Xenon lamp and a Peltier-cooled Hamamatsu R928P photomultiplier tube in photon-counting mode. Fully corrected emission spectra were obtained, for each compound, after excitation at the wavelength of the absorption maximum, with $A_{\lambda ex} < 0.1$ to minimize internal absorption. Quinine bisulfate in 0.5 M H_2SO_4 ($\Phi = 0.546$ at $\lambda_{ex} = 346$ nm) was used as a standard. Fluorescence lifetimes were measured by time correlated single-photon counting (TCSPC) by using the same FLS 920 fluorimeter. Excitation was achieved by a hydrogen-filled nanosecond flashlamp (repetition rate 40 kHz). The instrument response (FWHM ca. 1 ns) was determined by measuring the light scattered by a Ludox suspension. The TCSPC traces were analyzed by standard iterative reconvolution methods implemented in the software of the fluorimeter. All compounds displayed strictly monoexponential fluorescence decays.

4.8. Evaluation on kinases and molecular modeling experiments

The enzymatic activities of CDK2/Cyclin A, CDK5/p25, CDK9/Cyclin T, PIM1, CLK1, DYRK1A, GSK-3 isoforms α and/or β, CK1 isoforms δ/ε or ε, Haspin, ABL1, JAK3, Aurora B and Nek 6 kinases were assayed using the ADP-Glo™ bioluminescent kinase assay kit (Promega, Madison, WI) as previously described [16].

Geometric optimization of **6b** structures was obtained with Gaussian 09 [30] at the DFT level of theory using B3LYP functional and 6-31g basis set. The two helixes differ only in the values of two

dihedral angles defined by the following atoms (S2,C14,C15,C16) and (C14,C15,C16,C17). A scan of these two angles was performed to observe the transition state (TS) from one helix to another. TS was determined and optimized, and the intrinsic reaction coordinate (IRC) was calculated. The reagent and the product of the IRC were in turn optimized by taking into account the thermodynamic corrections for a final free Gibbs energy (ΔG) of 21.6 kcal.mol^{-1}.

The docking studies were performed with AutoDock Vina [34, 35]. Files for the docking were prepared from 3JPV PIM1 structure [33] after removing of water molecules, and **6b** and **HM107-g** pdbqt files were prepared with AutoDockTools (ADT) [57]. Apolar hydrogen atoms were removed and Gasteiger charges were added. Docking experiments were performed using the default AutoDock Vina parameters. The best docking solutions were submitted to molecular dynamics in the presence of solvent in order to appreciate the stability of the proposed solutions. The dynamics were realized using the NAMD software [58] and the Cgenff force field [59, 60].

4.9. Biological evaluation on cancer cell lines

The antiproliferative activity was studied in the A2058 (ATCC® CRL-11147) melanoma cell line as previously reported.[16]

Conflict of interest

There is no conflict of interest to declare.

Acknowledgments. We thank the Ministère de l'Enseignement supérieur et de la Recherche scientifique Algérien (M. N. B.-N.) and the Centre National de la Recherche Scientifique (F. M.). We acknowledge the Fonds Européen de Développement Régional (FEDER; D8 VENTURE Bruker AXS diffractometer) and Thermofisher (generous gift of 2,2,6,6-tetramethylpiperidine). L. P. and V. T. thank the French Cancer League (Comité 17) for financial support and the Cancéropôle Grand Ouest (axis:

natural sea products in cancer treatment) for scientific support. S. B. and S. R. also thank the Cancéropôle Grand Ouest (axis: natural sea products in cancer treatment), IBiSA (French *Infrastructures en sciences du vivant: biologie, santé et agronomie*) and Biogenouest (Western France life science and environment core facility network) for supporting KISS*f* screening facility. We also thank Frédéric Lassagne for his help all along the study. This research has been partly performed as part of the CNRS PICS project "Bimetallic synergy for the functionalization of heteroaromatics".

Supplementary data. Supplementary data associated with this article can be found online at http://doi.org/10.1016/j.bioorgxxxxxxxxxxx.

References and Notes

[1] A.M. Paiva, M.M. Pinto, E. Sousa, A century of thioxanthones: through synthesis and biological applications, Curr. Med. Chem. 20 (2013) 2438-2457, DOI: 10.2174/0929867311320190004.

[2] A. Palmeira, M.H. Vasconcelos, A. Paiva, M.X. Fernandes, M. Pinto, E. Sousa, Dual inhibitors of P-glycoprotein and tumor cell growth: (Re)discovering thioxanthones, Biochem. Pharmacol. 83 (2012) 57-68, DOI: 10.1016/j.bcp.2011.10.004.

[3] J. Barbosa, R.T. Lima, D. Sousa, A.S. Gomes, A. Palmeira, H. Seca, K. Choosang, P. Pakkong, H. Bousbaa, M.M. Pinto, E. Sousa, M.H. Vasconcelos, M. Pedro, Screening a small library of xanthones for antitumor activity and identification of a hit compound which induces apoptosis, Molecules 21 (2016) 81/81-81/15, DOI: 10.3390/molecules21010081.

[4] M. Hedidi, J. Maillard, W. Erb, F. Lassagne, Y.S. Halauko, O.A. Ivashkevich, V.E. Matulis, T. Roisnel, V. Dorcet, M. Hamzé, Z. Fajloun, B. Baratte, S. Ruchaud, S. Bach, G. Bentabed-Ababsa, F. Mongin, Fused systems based on 2-aminopyrimidines: Synthesis combining deprotolithiation-in situ zincation with N-arylation reactions and biological properties, Eur. J. Org. Chem. (2017) 5903-5915, DOI: 10.1002/ejoc.201701004.

[5] Y. Shin, S. Han, U. De, J. Park, S. Sharma, N.K. Mishra, E.-K. Lee, Y. Lee, H.S. Kim, I.S. Kim, Ru(II)-catalyzed selective C-H amination of xanthones and chromones with sulfonyl azides: Synthesis and anticancer evaluation, J. Org. Chem. 79 (2014) 9262-9271, DOI: 10.1021/jo501709f.

[6] D. Wagner, S. Bräse, Ruthenium-catalyzed C-H activation of thioxanthones, Beilstein J. Org. Chem. 11 (2015) 431-436, DOI: 10.3762/bjoc.11.49.

[7] S.H. Han, S. Kim, U. De, N.K. Mishra, J. Park, S. Sharma, J.H. Kwak, S. Han, H.S. Kim, I.S. Kim, Synthesis of succinimide-containing chromones, naphthoquinones, and xanthones under Rh(III) catalysis: Evaluation of anticancer activity, J. Org. Chem. 81 (2016) 12416-12425, DOI: 10.1021/acs.joc.6b02577.

[8] G. Tan, Q. You, J. You, Iridium-catalyzed oxidative heteroarylation of arenes and alkenes: Overcoming the restriction to specific substrates, ACS Catal. 8 (2018) 8709-8714, DOI: 10.1021/acscatal.8b02639.

[9] N. Mokhtari Brikci-Nigassa, G. Bentabed-Ababsa, W. Erb, F. Mongin, In situ 'trans-metal trapping': An efficient way to extend the scope of aromatic deprotometalation, Synthesis 50 (2018) 3615-3633, DOI: 10.1055/s-0036-1591953.

[10] M. Hedidi, W. Erb, F. Lassagne, Y.S. Halauko, O.A. Ivashkevich, V.E. Matulis, T. Roisnel, G. Bentabed-Ababsa, F. Mongin, Functionalization of pyridyl ketones using deprotolithiation-in situ zincation, RSC Adv. 6 (2016) 63185-63189, DOI: 10.1039/c6ra11370b.

[11] F. Lassagne, T. Langlais, E. Caytan, E. Limanton, L. Paquin, M. Boullard, C. Courtel, I. Curbet, C. Gédéon, J. Lebreton, L. Picot, V. Thiéry, M. Souab, B. Baratte, S. Ruchaud, S. Bach, T. Roisnel, F. Mongin, From quinoxaline, pyrido[2,3-*b*]pyrazine and pyrido[3,4-*b*]pyrazine to pyrazino-fused carbazoles and carbolines, Molecules 23 (2018) 2961/2961-2961/2922, DOI: 10.3390/molecules23112961.

[12] R. Amara, G. Bentabed-Ababsa, M. Hedidi, J. Khoury, H. Awad, E. Nassar, T. Roisnel, V. Dorcet, F. Chevallier, Z. Fajloun, F. Mongin, Synthesis of N-aryl and N-heteroaryl γ-, δ-, and ε-lactams using deprotometalation-iodination and N-arylation, and properties thereof, Synthesis 49 (2017) 4500-4516, DOI: 10.1055/s-0036-1590798.

[13] R.A. Altman, K.W. Anderson, S.L. Buchwald, Pyrrole-2-carboxylic acid as a ligand for the Cu-catalyzed reactions of primary anilines with aryl halides, J. Org. Chem. 73 (2008) 5167-5169, DOI: 10.1021/jo8008676.

[14] R.A. Altman, K.W. Anderson, S.L. Buchwald, Pyrrole-2-carboxylic acid as a ligand for the Cu-catalyzed reactions of primary anilines with aryl halides, J. Org. Chem. 73 (2008) 5167-5169, DOI: 10.1021/jo8008676.

[15] H. Fujiwara, K. Kitagawa, Synthesis of [1]benzopyrano[2,3,4-kl]acridin-3-ol and its analogs as pentacyclic compounds, Chem. Pharm. Bull. 48 (2000) 1380-1383, DOI: 10.1248/cpb.48.1380.

[16] N. Mokhtari Brikci-Nigassa, G. Bentabed-Ababsa, W. Erb, F. Chevallier, L. Picot, L. Vitek, A. Fleury, V. Thiéry, M. Souab, T. Robert, S. Ruchaud, S. Bach, T. Roisnel, F. Mongin, 2-Aminophenones, a common precursor to N-aryl isatins and acridines endowed with bioactivities, Tetrahedron 74 (2018) 1785-1801, DOI: 10.1016/j.tet.2018.02.038.

[17] J. Kim, S. Chang, Ammonium salts as an inexpensive and convenient nitrogen source in the Cu-catalyzed amination of aryl halides at room temperature, Chem. Commun. (2008) 3052-3054, DOI: 10.1039/b804637a.

[18] P. Ji, J.H. Atherton, M.I. Page, Copper(I)-catalyzed amination of aryl halides in liquid ammonia, J. Org. Chem. 77 (2012) 7471-7478, DOI: 10.1021/jo301204t.

[19] H.S. Jung, T. Yun, Y. Cho, H.B. Jeon, Simple and convenient copper-catalyzed amination of aryl halides to primary arylamines using NH_4OH, Tetrahedron 72 (2016) 5988-5993, DOI: 10.1016/j.tet.2016.07.021.

[20] Y. Kitahara, T. Mizuno, A. Kubo, Synthetic studies of benzo[b]pyrrolo[4,3,2-de][1,10]phenanthroline, Tetrahedron 60 (2004) 4283-4288, DOI: 10.1016/j.tet.2004.03.057.

[21] S. Klaeger, S. Heinzlmeir, M. Wilhelm, H. Polzer, B. Vick, P.-A. Koenig, M. Reinecke, B. Ruprecht, S. Petzoldt, C. Meng, J. Zecha, K. Reiter, H. Qiao, D. Helm, H. Koch, M. Schoof, G. Canevari, E. Casale, S.R. Depaolini, A. Feuchtinger, Z. Wu, T. Schmidt, L. Rueckert, W. Becker, J. Huenges, A.-K. Garz, B.-O. Gohlke, D.P. Zolg, G. Kayser, T. Vooder, R. Preissner, H. Hahne, N. Tonisson, K. Kramer, K. Goetze, F. Bassermann, J. Schlegl, H.-C. Ehrlich, S. Aiche, A. Walch, P.A. Greif, S. Schneider, E.R. Felder, J. Ruland, G. Medard, I. Jeremias, K. Spiekermann, B. Kuster, The target landscape of clinical kinase drugs, Science 358 (2017) 1148, DOI: 10.1126/science.aan4368.

[22] R. Roskoski, Jr., Properties of FDA-approved small molecule protein kinase inhibitors, Pharmacol. Res. 144 (2019) 19-50, DOI: 10.1016/j.phrs.2019.03.006.

[23] H.L. Lightfoot, F.W. Goldberg, J. Sedelmeier, Evolution of Small Molecule Kinase Drugs, ACS Medicinal Chemistry Letters 10 (2019) 153-160, DOI: 10.1021/acsmedchemlett.8b00445.

[24] L.S. Chen, S. Redkar, D. Bearss, W.G. Wierda, V. Gandhi, Pim kinase inhibitor, SGI-1776, induces apoptosis in chronic lymphocytic leukemia cells, Blood 114(19) (2009) 4150-4157, DOI: 10.1182/blood-2009-03-212852.

[25] V.J. Cee, F. Chavez, B. Herberich, B.A. Lanman, L.H. Pettus, A.B. Reed, B. Wu, R.P. Wurz, K.L. Andrews, J. Chen, D. Hickman, J. Laszlo, M.R. Lee, N. Guerrero, B.K. Mattson, Y. Nguyen, C. Mohr, K. Rex, C.E. Sastri, P. Wang, Q. Wu, T. Wu, Y. Xu, Y. Zhou, J.T. Winston, J.R. Lipford, A.S. Tasker, H.-L. Wang, Discovery and Optimization of Macrocyclic Quinoxaline-pyrrolo-dihydropiperidinones as Potent Pim-1/2 Kinase Inhibitors, ACS Medicinal Chemistry Letters 7(4) (2016) 408-412, DOI: 10.1021/acsmedchemlett.5b00403.

[26] C.J.R. Bataille, M.B. Brennan, S. Byrne, S.G. Davies, M. Durbin, O. Fedorov, K.V.M. Huber, A.M. Jones, S. Knapp, G. Liu, A. Nadali, C.E. Quevedo, A.J. Russell, R.G. Walker, R. Westwood, G.M. Wynne, Thiazolidine derivatives as potent and selective inhibitors of the PIM kinase family, Bioorg. Med. Chem. 25(9) (2017) 2657-2665, DOI: 10.1016/j.bmc.2017.02.056.

[27] Y. Shen, C.-F. Chen, Helicenes: Synthesis and Applications, Chem. Rev. 112 (2012) 1463-1535, DOI: 10.1021/cr200087r.

[28] M. Gingras, One hundred years of helicene chemistry. Part 3: applications and properties of carbohelicenes, Chem. Soc. Rev. 42 (2013) 1051-1095, DOI: 10.1039/c2cs35134j.

[29] R.H. Janke, G. Haufe, E.-U. Würthwein, J.H. Borkent, Racemization barriers of helicenes: A computational study, J. Am. Chem. Soc. 118 (1996) 6031-6035, DOI: 10.1021/ja950774t.

[30] M.J. Frisch, G.W. Trucks, H.B. Schlegel, G.E. Scuseria, M.A. Robb, J.R. Cheeseman, G. Scalmani, V. Barone, B. Mennucci, G.A. Petersson, H. Nakatsuji, M. Caricato, X. Li, H.P. Hratchian, A.F. Izmaylov, J. Bloino, G. Zheng, J.L. Sonnenberg, M. Hada, M. Ehara, K. Toyota, R. Fukuda, J. Hasegawa, M. Ishida, T. Nakajima, Y. Honda, O. Kitao, H. Nakai, T. Vreven, J.A. Montgomery Jr., J.E. Peralta, F. Ogliaro, M. Bearpark, J.J. Heyd, E. Brothers, K.N. Kudin, V.N. Staroverov, R. Kobayashi, J. Normand, K. Raghavachari, A. Rendell, J.C. Burant, S.S. Iyengar, J. Tomasi, M. Cossi, N. Rega, M.J. Millam, M. Klene, J.E. Knox, J.B. Cross, V. Bakken, C. Adamo, J. Jaramillo, R. Gomperts, R.E. Stratmann, O. Yazyev, A.J. Austin, R. Cammi, C. Pomelli, J.W. Ochterski, R.L. Martin, K. Morokuma, V.G. Zakrzewski, G.A. Voth, P. Salvador, J.J. Dannenberg, S. Dapprich, A.D. Daniels, Ö. Farkas, J.B. Foresman, J.V. Ortiz, J. Cioslowski, D.J. Fox, Gaussian 09, Revision D.01, Gaussian Inc., Wallingford CT, 2009.

[31] C. Goedicke, H. Stegemeyer, Resolution and racemization of pentahelicene, Tetrahedron Lett. (1970) 937-940, DOI: 10.1016/s0040-4039(01)97871-2.

[32] T. Katayama, S. Nakatsuka, H. Hirai, N. Yasuda, J. Kumar, T. Kawai, T. Hatakeyama, Two-step synthesis of boron-fused double helicenes, J. Am. Chem. Soc. 138 (2016) 5210-5213, DOI: 10.1021/jacs.6b01674.

[33] R. Akué-Gédu, E. Rossignol, S. Azzaro, S. Knapp, P. Filippakopoulos, A.N. Bullock, J. Bain, P. Cohen, M. Prudhomme, F. Anizon, P. Moreau, Synthesis, Kinase Inhibitory Potencies, and in Vitro Antiproliferative Evaluation of New Pim Kinase Inhibitors, J. Med. Chem. 52 (2009) 6369-6381, DOI: 10.1021/jm901018f.

[34] G.M. Morris, R. Huey, W. Lindstrom, M.F. Sanner, R.K. Belew, D.S. Goodsell, A.J. Olson, AutoDock and AutoDockTools: Automated docking with selective receptor flexibility, J. Comput. Chem. 30 (2009) 2785-2791, DOI: 10.1002/jcc.21256.

[35] O. Trott, A.J. Olson, AutoDock Vina: Improving the speed and accuracy of docking with a new scoring function, efficient optimization, and multithreading, J. Comput. Chem. 31 (2010) 455-461, DOI: 10.1002/jcc.21334.

[36] V. Pogacic, A.N. Bullock, O. Fedorov, P. Filippakopoulos, C. Gasser, A. Biondi, S. Meyer-Monard, S. Knapp, J. Schwaller, Structural analysis identifies imidazo[1,2-b]pyridazines as PIM kinase inhibitors with in vitro antileukemic activity, Cancer Res. 67 (2007) 6916-6924, DOI: 10.1158/0008-5472.can-07-0320.

[37] X. Wang, W. Blackaby, V. Allen, G.K.Y. Chan, J.H. Chang, P.-C. Chiang, C. Diene, J. Drummond, S. Do, E. Fan, E.B. Harstad, A. Hodges, H. Hu, W. Jia, W. Kofie, A. Kolesnikov, J.P. Lyssikatos, J. Ly, M. Matteucci, J.G. Moffat, V. Munugalavadla, J. Murray, D. Nash, C.L. Noland, G. Del Rosario, L. Ross, C. Rouse, A. Sharpe, D. Slaga, M. Sun, V. Tsui, H. Wallweber, S.-F. Yu, A.J. Ebens, Optimization of Pan-Pim Kinase Activity and Oral Bioavailability Leading to Diaminopyrazole (GDC-0339) for the Treatment of Multiple Myeloma, J. Med. Chem. 62 (2019) 2140-2153, DOI: 10.1021/acs.jmedchem.8b01857.

[38] X. Wang, A. Kolesnikov, S. Tay, G. Chan, Q. Chao, S. Do, J. Drummond, A.J. Ebens, N. Liu, J. Ly, E. Harstad, H. Hu, J. Moffat, V. Munugalavadla, J. Murray, D. Slaga, V. Tsui, M. Volgraf, H. Wallweber, J.H. Chang, Discovery of 5-azaindazole (GNE-955) as a potent pan-Pim inhibitor with optimized bioavailability, J. Med. Chem. 60 (2017) 4458-4473, DOI: 10.1021/acs.jmedchem.7b00418.

[39] E.F. Pettersen, T.D. Goddard, C.C. Huang, G.S. Couch, D.M. Greenblatt, E.C. Meng, T.E. Ferrin, UCSF Chimera-A visualization system for exploratory research and analysis, J. Comput. Chem. 25 (2004) 1605-1612, DOI: 10.1002/jcc.20084.

[40] Y. Zhang, Z. Wang, X. Li, N.S. Magnuson, Pim kinase-dependent inhibition of c-Myc degradation, Oncogene 27(35) (2008) 4809-4819, DOI: 10.1038/onc.2008.123.

[41] N.M. Santio, S.K.-J. Landor, L. Vahtera, J. Ylä-Pelto, E. Paloniemi, S.Y. Imanishi, G. Corthals, M. Varjosalo, G.B. Manoharan, A. Uri, U. Lendahl, C. Sahlgren, P.J. Koskinen, Phosphorylation of Notch1 by Pim kinases promotes oncogenic signaling in breast and prostate cancer cells, Oncotarget 7(28) (2016) 43220-43238, DOI: 10.18632/oncotarget.9215.

[42] D. Horiuchi, R. Camarda, A.Y. Zhou, C. Yau, O. Momcilovic, S. Balakrishnan, A.N. Corella, H. Eyob, K. Kessenbrock, D.A. Lawson, L.A. Marsh, B.N. Anderton, J. Rohrberg, R. Kunder, A.V. Bazarov, P. Yaswen, M.T. McManus, H.S. Rugo, Z. Werb, A. Goga, PIM1 kinase inhibition as a targeted therapy against triple-negative breast tumors with elevated MYC expression, Nat. Med. 22(11) (2016) 1321-1329, DOI: 10.1038/nm.4213.

[43] N.M. Santio, R.L. Vahakoski, E.-M. Rainio, J.A. Sandholm, S.S. Virtanen, M. Prudhomme, F. Anizon, P. Moreau, P. Koskinen, J., Pim-selective inhibitor DHPCC-9 reveals Pim kinases as potent stimulators of cancer cell migration and invasion, Molecular cancer 9 (2010) 279, DOI: 10.1186/1476-4598-9-279.

[44] C. Locatelli, F.B. Filippin-Monteiro, T.B. Creczynski, Recent advances in the biology, therapy and management of melanoma, L. Davids, ed., InTech, 2013.

[45] B. Shannan, A. Watters, Q. Chen, S. Mollin, M. Dörr, E. Meggers, X. Xu, P. Gimotty, A., M. Perego, L. Li, J. Benci, C. Krepler, P. Brafford, J. Zhang, Z. Wei, G. Zhang, Q. Liu, X. Yin, K. Nathanson, L., M. Herlyn, A. Vultur, PIM kinases as therapeutic targets against advanced melanoma, Oncotarget 7(34) (2016) 54897-54912, DOI: 10.18632/oncotarget.10703.

[46] J. Wu, J. Du, X. Fu, B. Liu, H. Cao, T. Li, T. Su, J. Xu, A. Kai-Wing Tse, Z.-L. Yu, Iciartin, a novel FASN inhibitor, exerts anti-melanoma activities through IGF-1R/STAT3 signaling, Oncotarget 7(32) (2016) 51251-51269, DOI: 10.18632/oncotarget.9984.

[47] H.E. Gottlieb, V. Kotlyar, A. Nudelman, NMR chemical shifts of common laboratory solvents as trace impurities, J. Org. Chem. 62 (1997) 7512-7515, DOI: 10.1021/jo971176v.

[48] R.A. Kjonaas, R.K. Hoffer, Regiospecific 1,4-addition with Grignard-derived mixed triorganozincate reagents, J. Org. Chem. 53 (1988) 4133-4135, DOI: 10.1021/jo00252a055.

[49] A.I. Vogel, A.R. Tatchell, B.S. Furnis, A.J. Hannaford, P.W.G. Smith, Vogel's textbook of practical organic chemistry, 5th edn, Prentice Hall, 1996.

[50] J.M. L'Helgoual'ch, A. Seggio, F. Chevallier, M. Yonehara, E. Jeanneau, M. Uchiyama, F. Mongin, Deprotonative Metalation of Five-membered Aromatic Heterocycles using Mixed Lithium-zinc Species, J. Org. Chem. 73 (2008) 177-183, DOI: 10.1021/jo7020345.

[51] M. Hedidi, G. Bentabed-Ababsa, A. Derdour, T. Roisnel, V. Dorcet, F. Chevallier, L. Picot, V. Thiéry, F. Mongin, Synthesis of C,N'-linked bis-heterocycles using a deprotometalation-

iodination-N-arylation sequence and evaluation of their antiproliferative activity in melanoma cells, Bioorg. Med. Chem. 22 (2014) 3498-3507, DOI: 10.1016/j.bmc.2014.04.028.
[52] G.M. Sheldrick, SHELXT - Integrated space-group and crystal-structure determination, Acta Crystallogr., Sect. A 71 (2015) 3-8, DOI: 10.1107/s2053273314026370.
[53] G.M. Sheldrick, Crystal structure refinement with SHELXL, Acta Crystallogr., Sect. C 71 (2015) 3-8, DOI: 10.1107/s2053229614024218.
[54] L.J. Farrugia, ORTEP-3 for windows - a version of ORTEP-III with a graphical user interface (GUI), J. Appl. Crystallogr. 30 (1997) 565, DOI: 10.1107/S0021889897003117.
[55] F. Mayer, Derivatives of thiosalicylic acid and of thioxanthone, Ber. Dtsch. Chem. Ges. 42 (1909) 3046-3067, DOI: 10.1002/cber.19090420323.
[56] Y. Liu, H. Chen, X. Hu, W. Zhou, G.-J. Deng, Selenium-promoted intramolecular oxidative amidation of 2-(arylamino)acetophenones for the synthesis of N-arylisatins, Eur. J. Org. Chem. 2013 (2013) 4229-4232, DOI: 10.1002/ejoc.201300477.
[57] M.F. Sanner, Python: A programming language for software integration and development, J. Mol. Graphics Modell. 17 (1999) 57-61.
[58] J.C. Phillips, R. Braun, W. Wang, J. Gumbart, E. Tajkhorshid, E. Villa, C. Chipot, R.D. Skeel, L. Kale, K. Schulten, Scalable molecular dynamics with NAMD, J. Comput. Chem. 26 (2005) 1781-1802, DOI: 10.1002/jcc.20289.
[59] K. Vanommeslaeghe, E. Hatcher, C. Acharya, S. Kundu, S. Zhong, J. Shim, E. Darian, O. Guvench, P. Lopes, I. Vorobyov, A.D. Mackerell, Jr., CHARMM general force field: A force field for drug-like molecules compatible with the CHARMM all-atom additive biological force fields, J. Comput. Chem. 31 (2010) 671-690, DOI: 10.1002/jcc.21367.
[60] W. Yu, X. He, K. Vanommeslaeghe, A.D. MacKerell, Extension of the CHARMM general force field to sulfonyl-containing compounds and its utility in biomolecular simulations, J. Comput. Chem. 33 (2012) 2451-2468, DOI: 10.1002/jcc.23067.